US 20250258369A1

(19) United States

(12) Patent Application Publication

(10) Pub. No.: US 2025/0258369 A1

(43) Pub. Date: Aug. 14, 2025

TERAMURA et al.

(54) **LIGHT SCANNING APPARATUS AND IMAGE FORMING APPARATUS**

(71) Applicant: **CANON KABUSHIKI KAISHA**, Tokyo (JP)

(72) Inventors: **MASAYASU TERAMURA**, Tochigi (JP); **SOYA SAIJO**, Tochigi (JP)

(21) Appl. No.: **19/041,774**

(22) Filed: **Jan. 30, 2025**

(30) **Foreign Application Priority Data**

Feb. 13, 2024 (JP) 2024-019123

Publication Classification

(51) **Int. Cl.**

G02B 26/12 (2006.01)
G02B 26/10 (2006.01)
G03G 15/043 (2006.01)

(52) **U.S. Cl.**

CPC ***G02B 26/124*** (2013.01); ***G02B 26/105*** (2013.01); ***G02B 26/125*** (2013.01); ***G03G 15/0435*** (2013.01)

(57) **ABSTRACT**

Provided is an apparatus in which a distance between a light source and a deflecting surface of a deflecting unit on an optical axis of an incident system, a distance between the deflecting surface and a sagittal line tilt surface of an imaging element on an optical axis of the imaging element, a lateral magnification in a sub-scanning cross section of the incident system, and an inclination of the sagittal line tilt surface at a position at which a light flux from each light emitting point of the light source arrives on the sagittal line tilt surface are appropriately set.

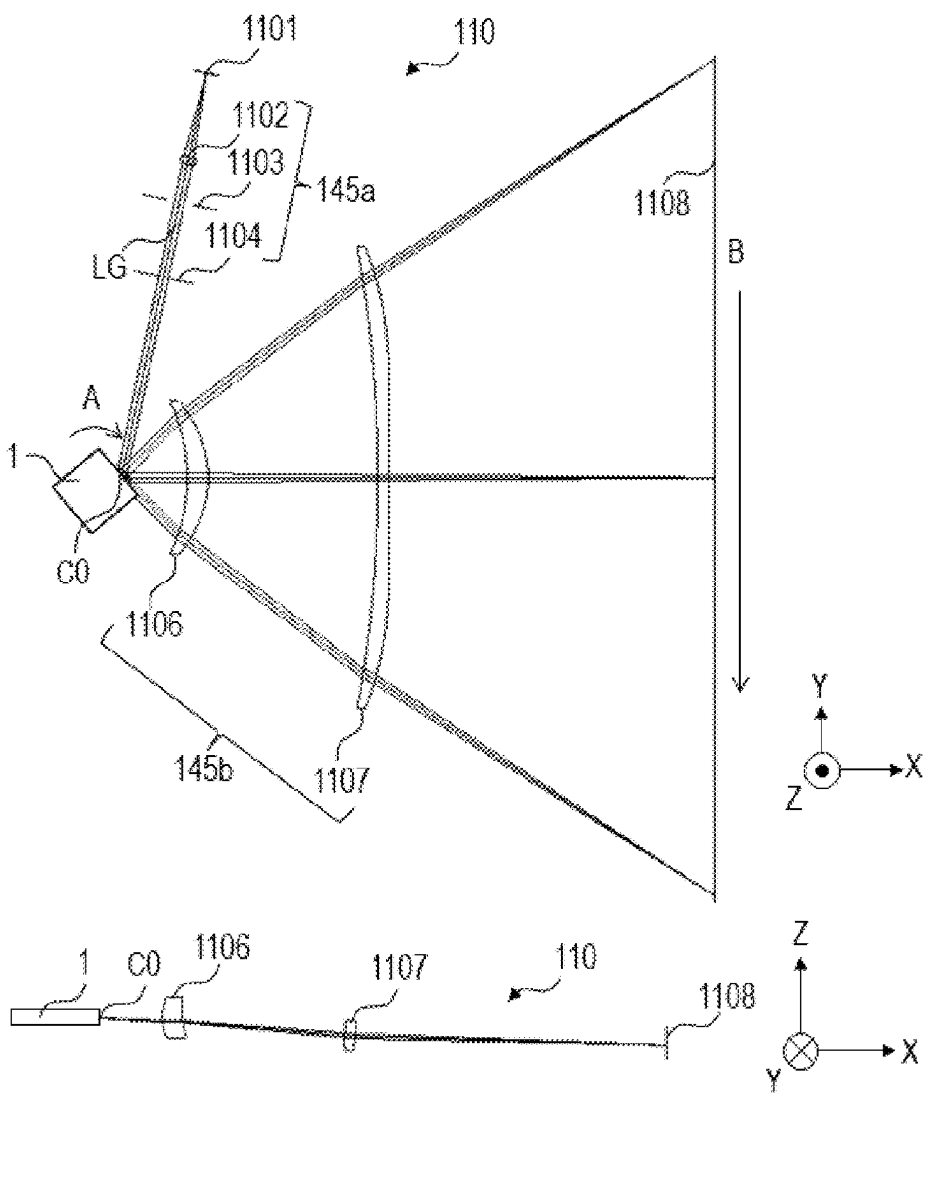

FIG. 1A

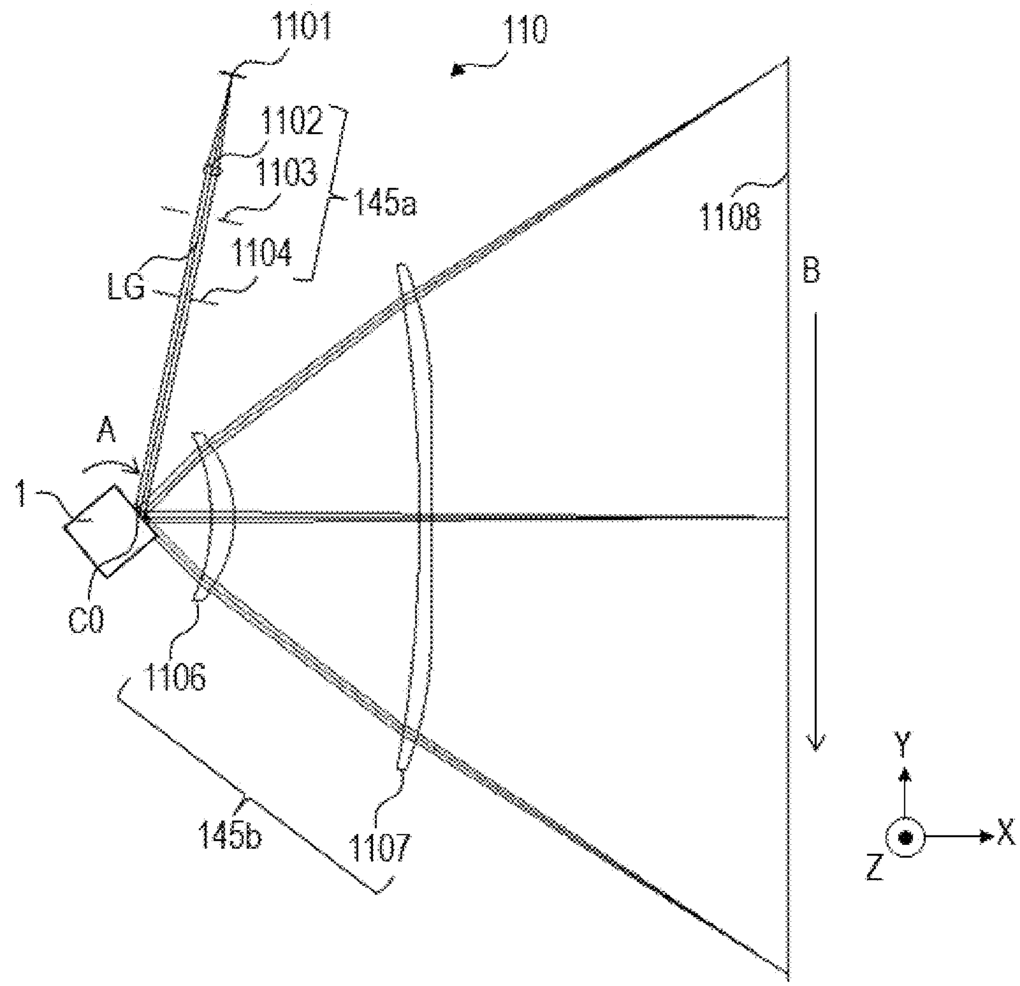

FIG. 1B


1
C0
1106
1107
110
1108
Z
X
Y

FIG. 2

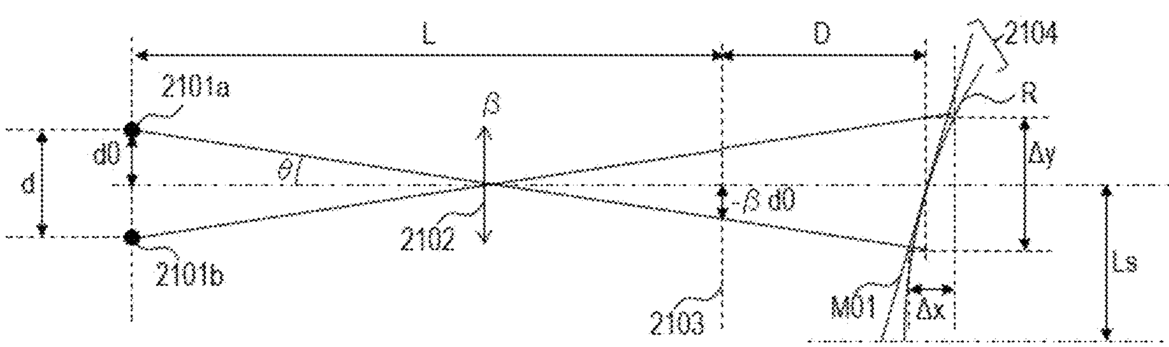
L
D
2104
2101a
R
β
d0
Δy
d
θ
-β d0
Ls
2102
2101b
2103
M01
Δx

FIG. 3A

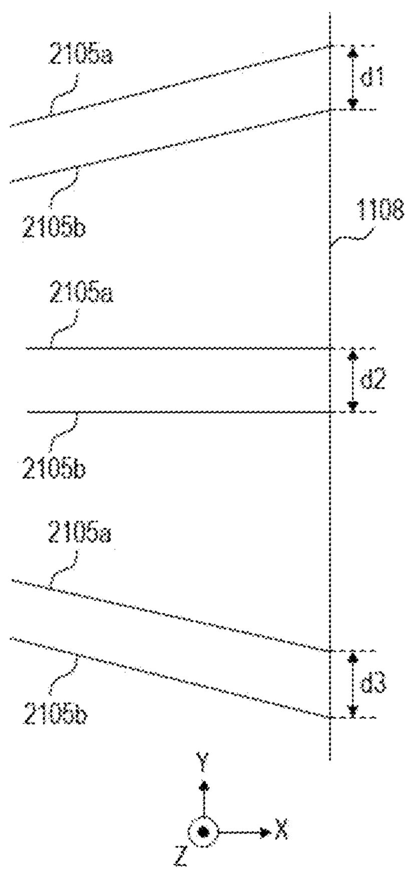
2105a
d1
2105b
1108
2105a
d2
2105b
2105a
d3
2105b
Y
X
Z

FIG. 3B

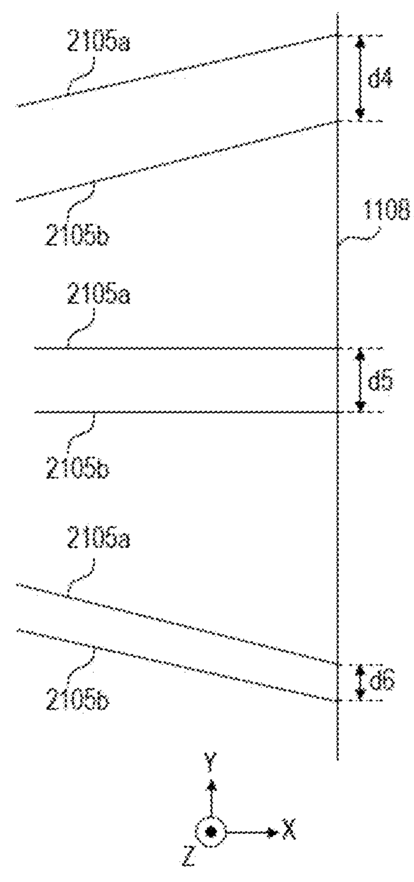
2105a
d4
2105b
1108
2105a
d5
2105b
2105a
d6
2105b
Y
X
Z

FIG. 4

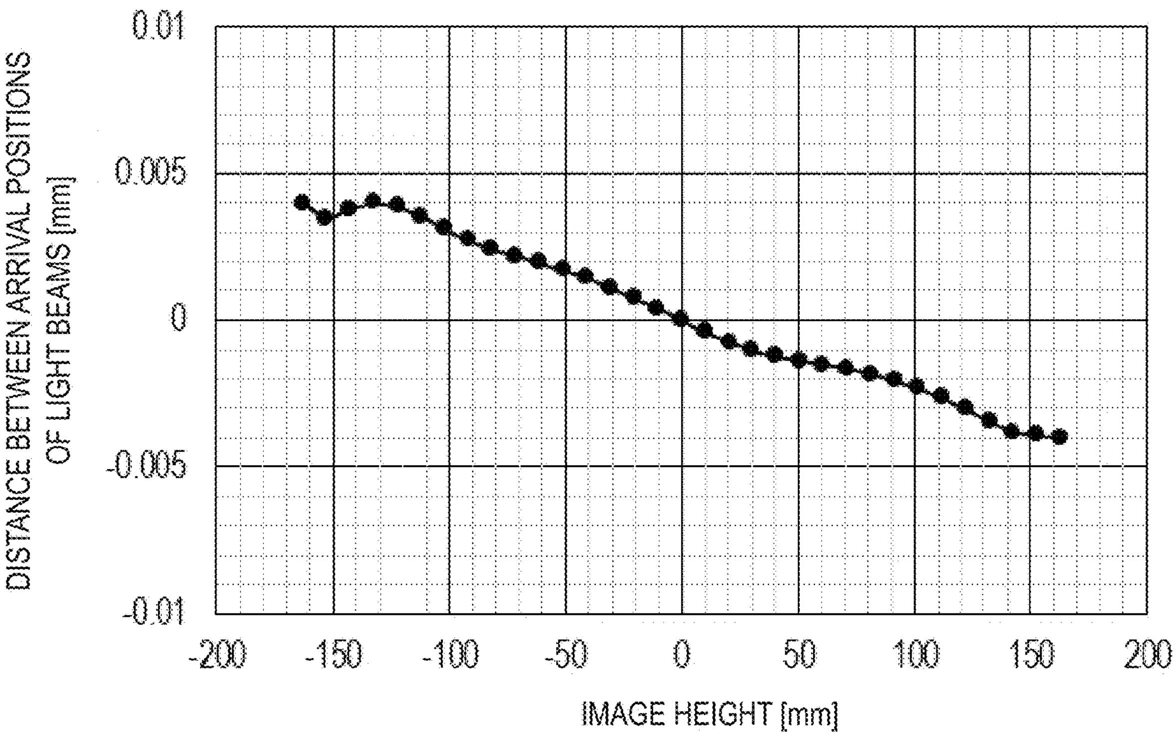
0.01
0.005
0
-0.005
-0.01
DISTANCE BETWEEN ARRIVAL POSITIONS OF LIGHT BEAMS [mm]
-200
-150
-100
-50
0
50
100
150
200
IMAGE HEIGHT [mm]

FIG. 5A

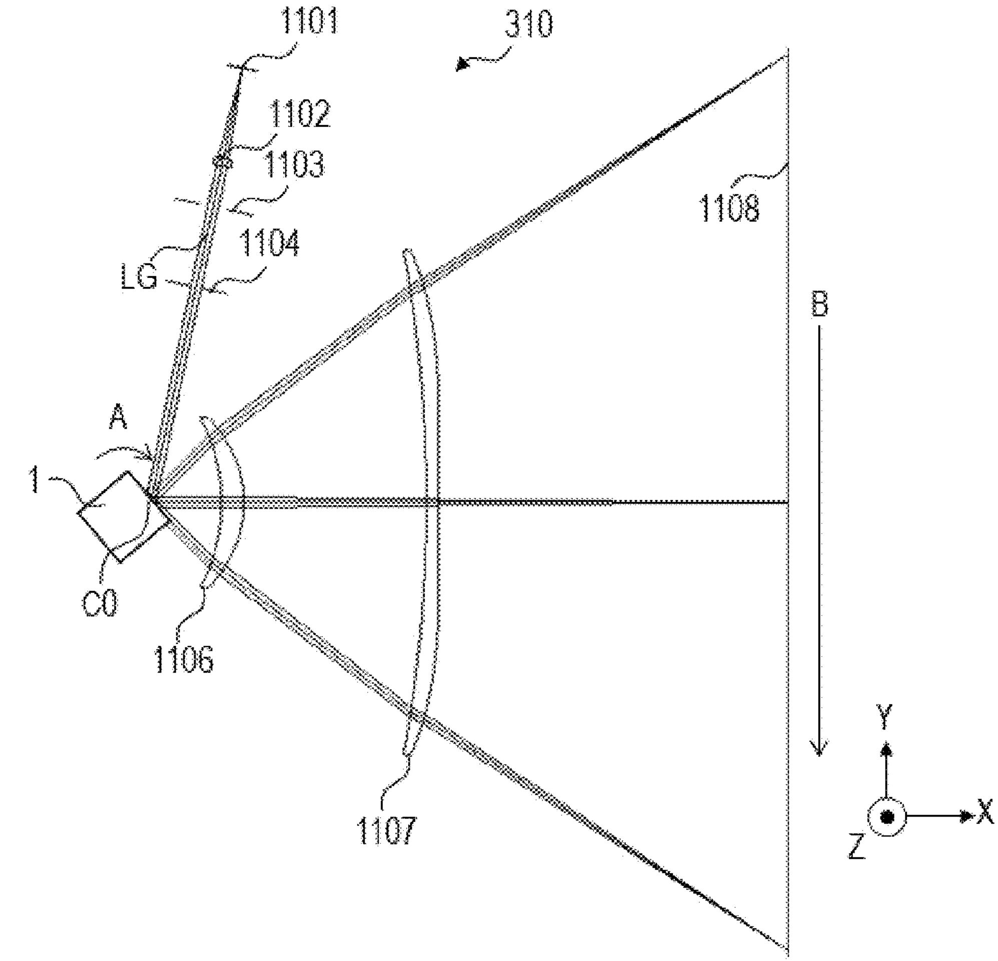
1101
310
1102
1103
1108
LG
1104
B
A
1
C0
1106
Y
X
Z
1107

FIG. 5B

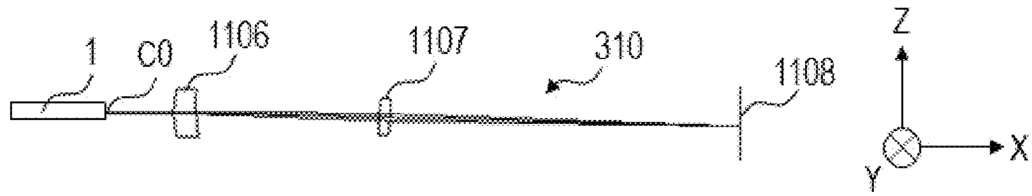
1
C0
1106
1107
310
1108
Z
X
Y

FIG. 6

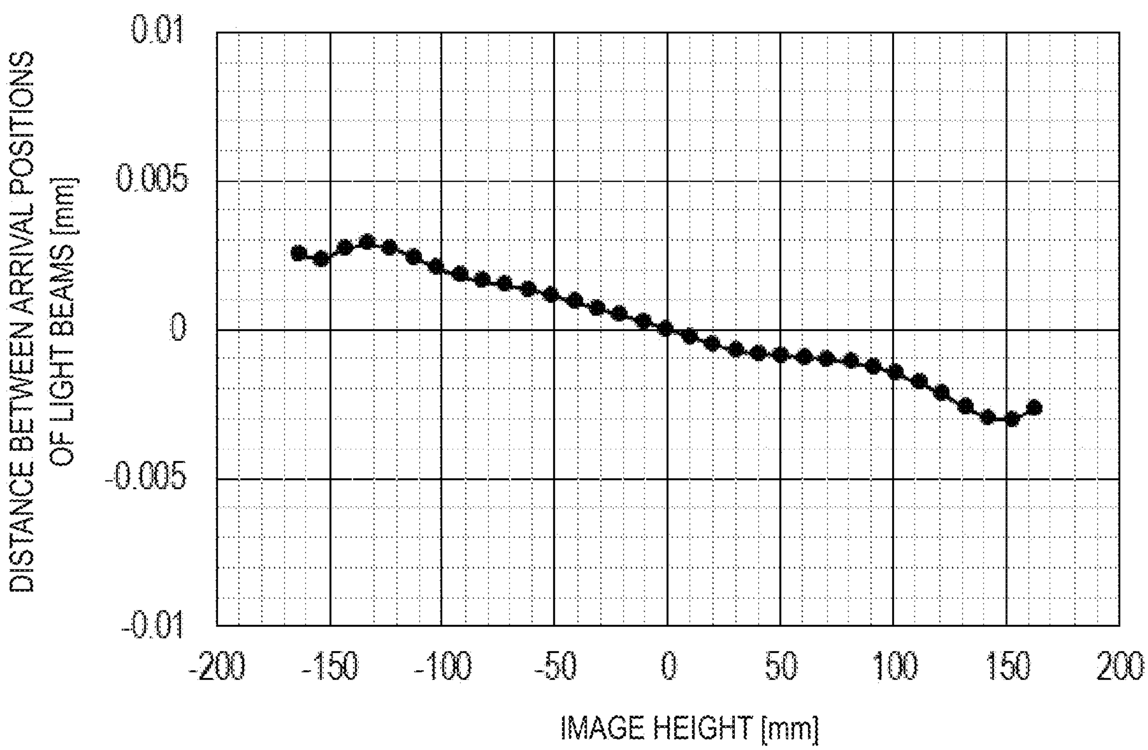

0.01
0.005
0
-0.005
-0.01
DISTANCE BETWEEN ARRIVAL POSITIONS OF LIGHT BEAMS [mm]
-200
-150
-100
-50
0
50
100
150
200
IMAGE HEIGHT [mm]

FIG. 7A

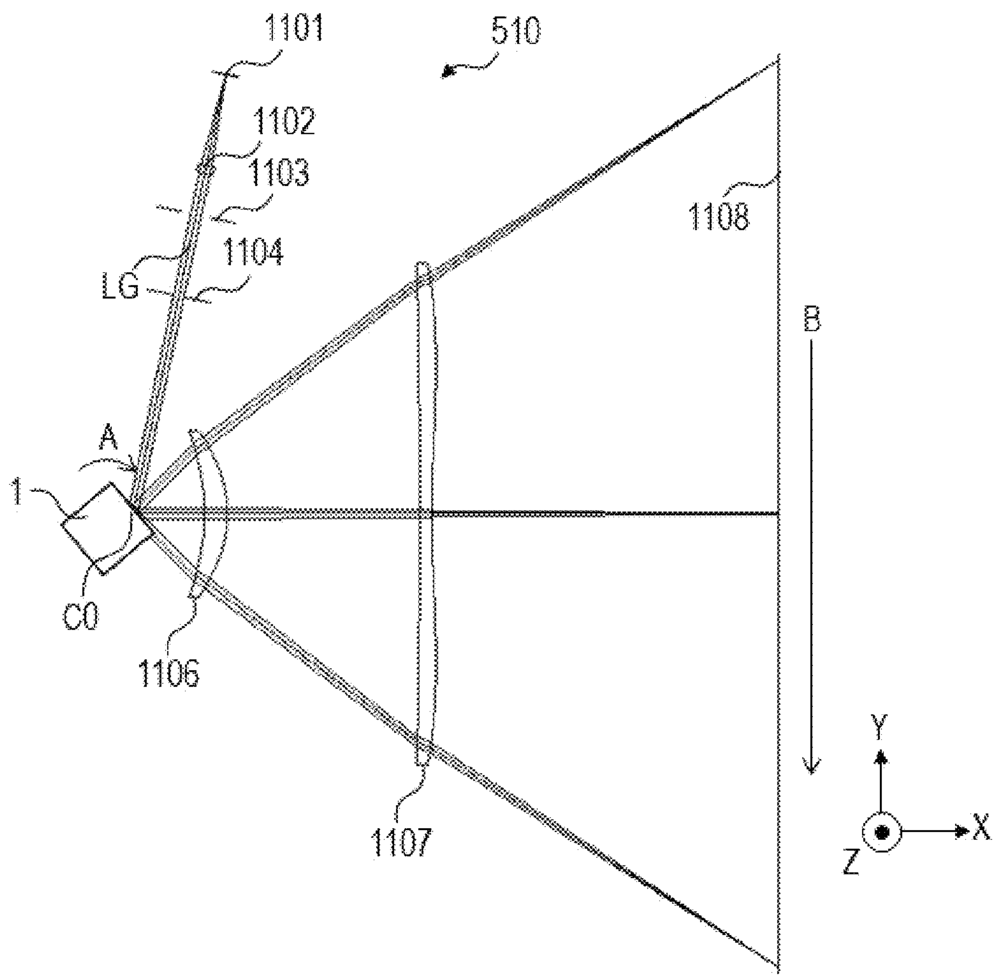
1101
510
1102
1103
1104
LG
1108
B
A
1
C0
1106
1107
Y
X
Z

FIG. 7B

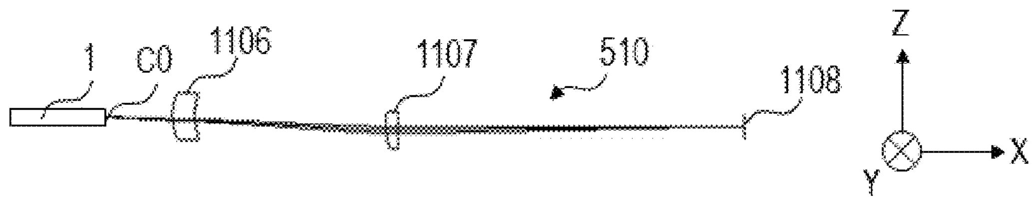
1
C0
1106
1107
510
1108
Z
X
Y

FIG. 8

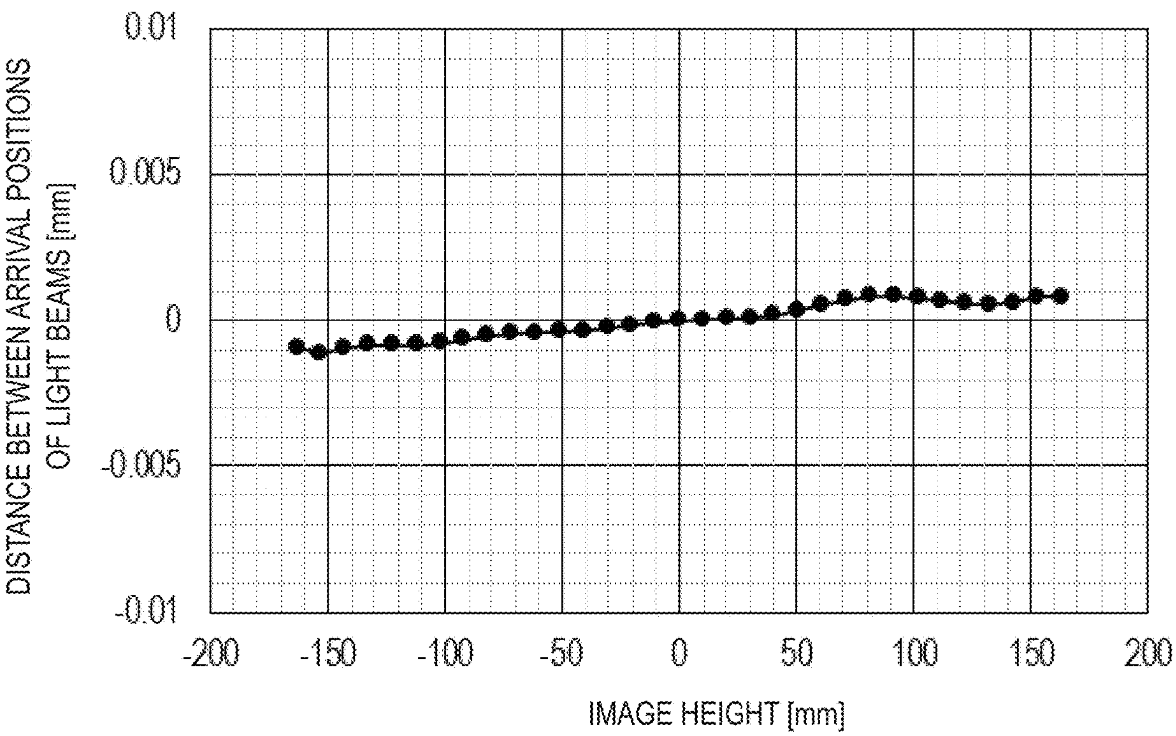

0.01
0.005
0
-0.005
-0.01
DISTANCE BETWEEN ARRIVAL POSITIONS OF LIGHT BEAMS [mm]
-200
-150
-100
-50
0
50
100
150
200
IMAGE HEIGHT [mm]

FIG. 9A

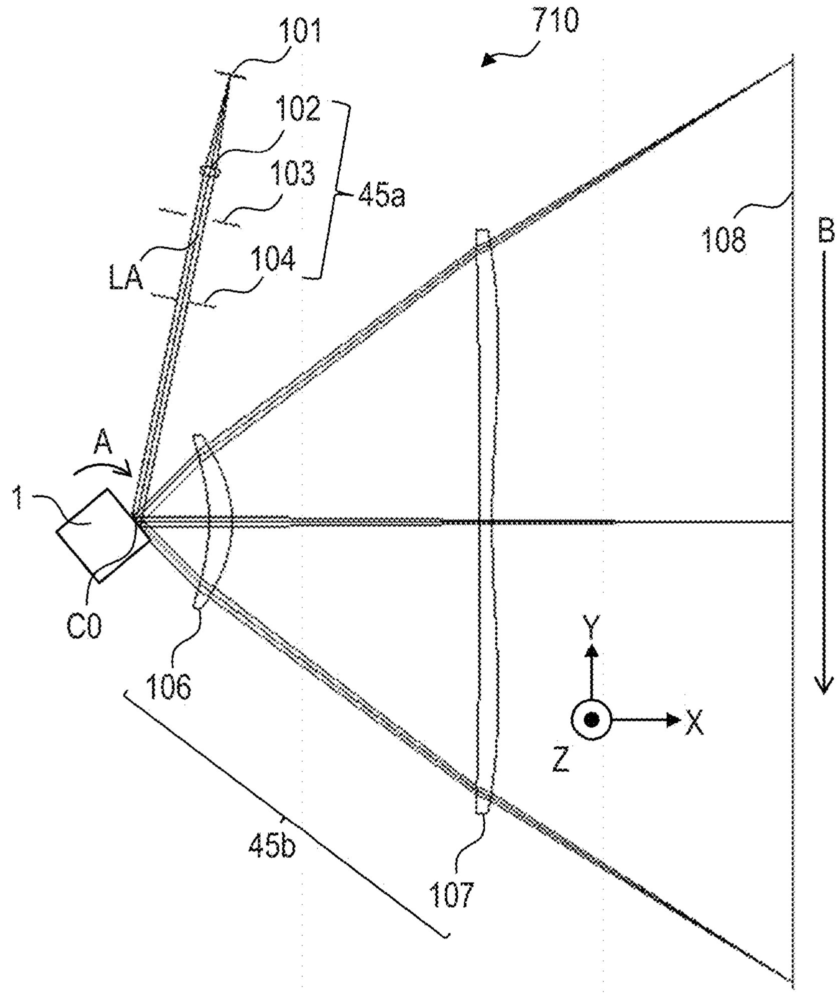

FIG. 9B

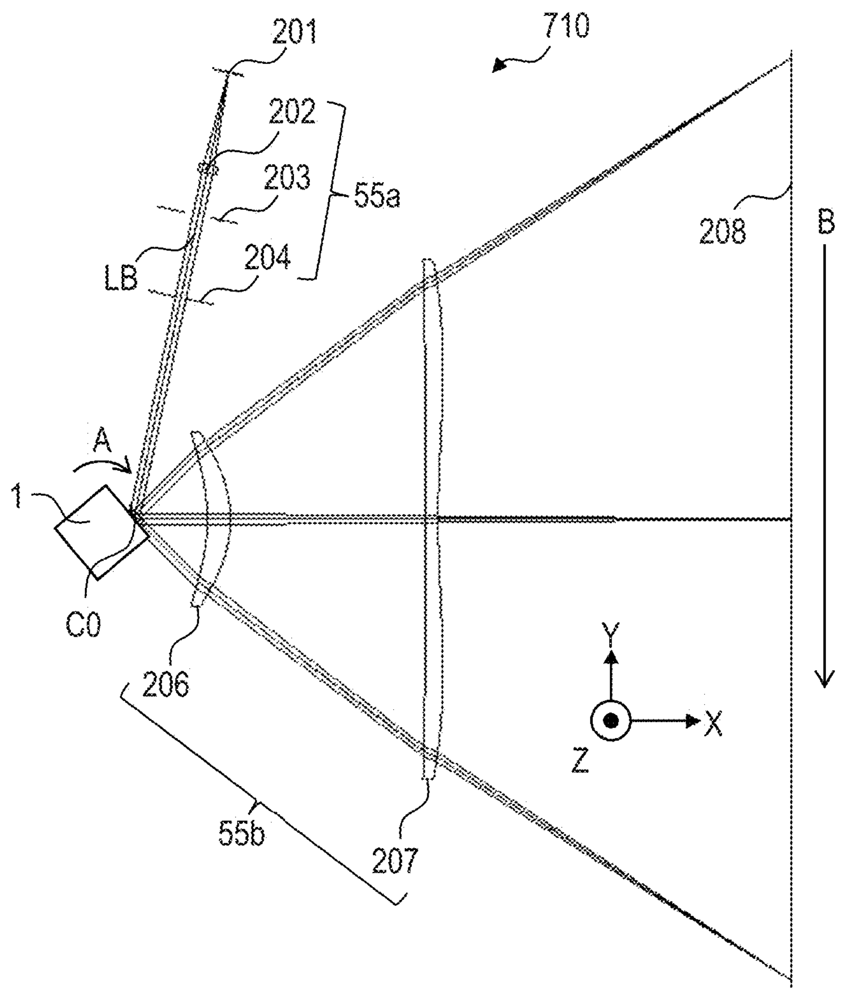

FIG. 10

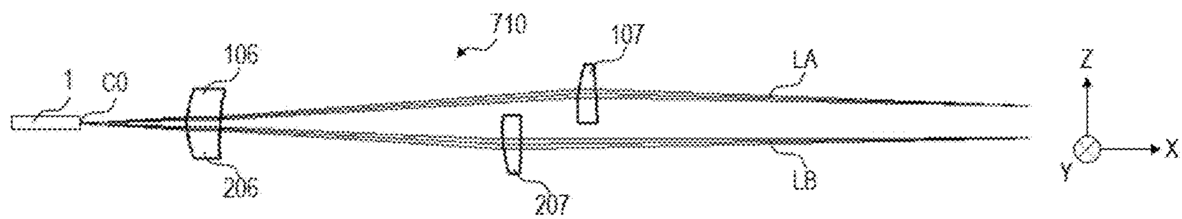
710
106
107
LA
Z
1
C0
X
Y
206
LB
207

FIG. 11

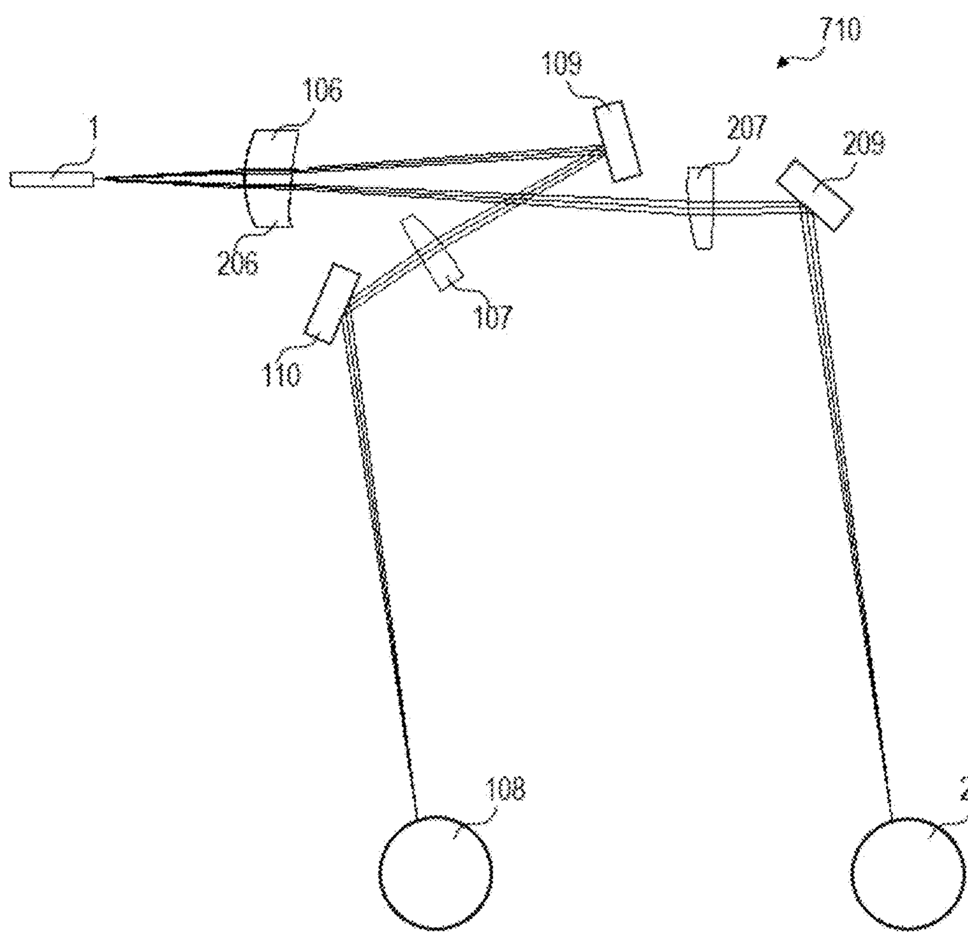
710
109
106
207
209
1
206
107
110
108
208

FIG. 12A

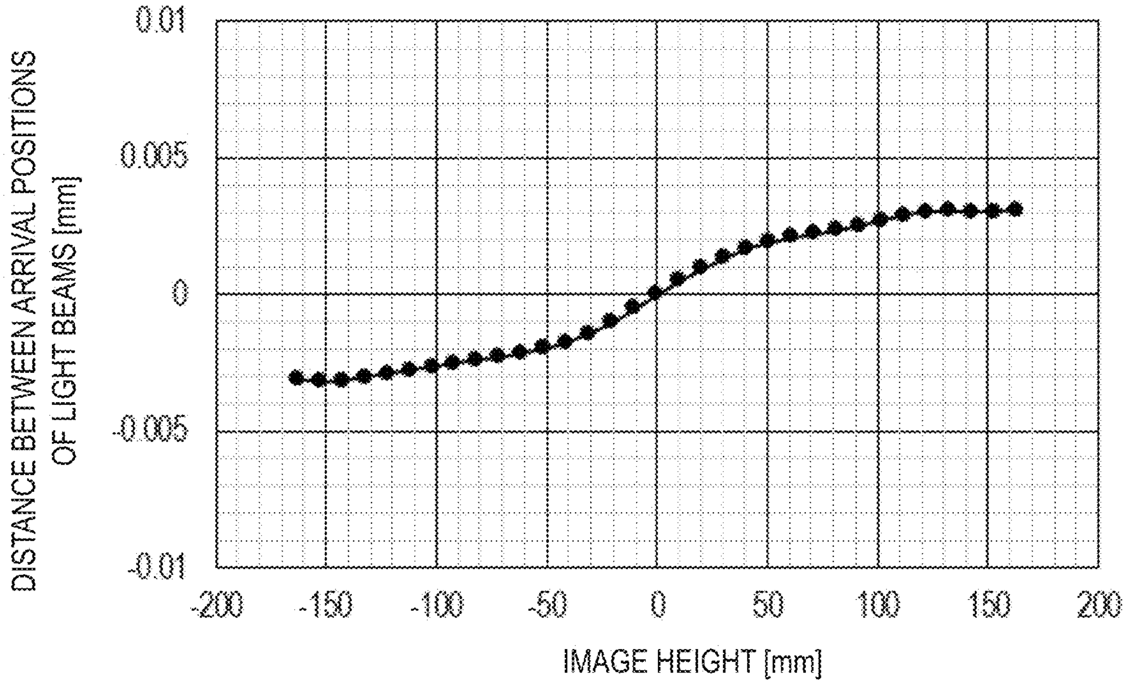

FIG. 12B

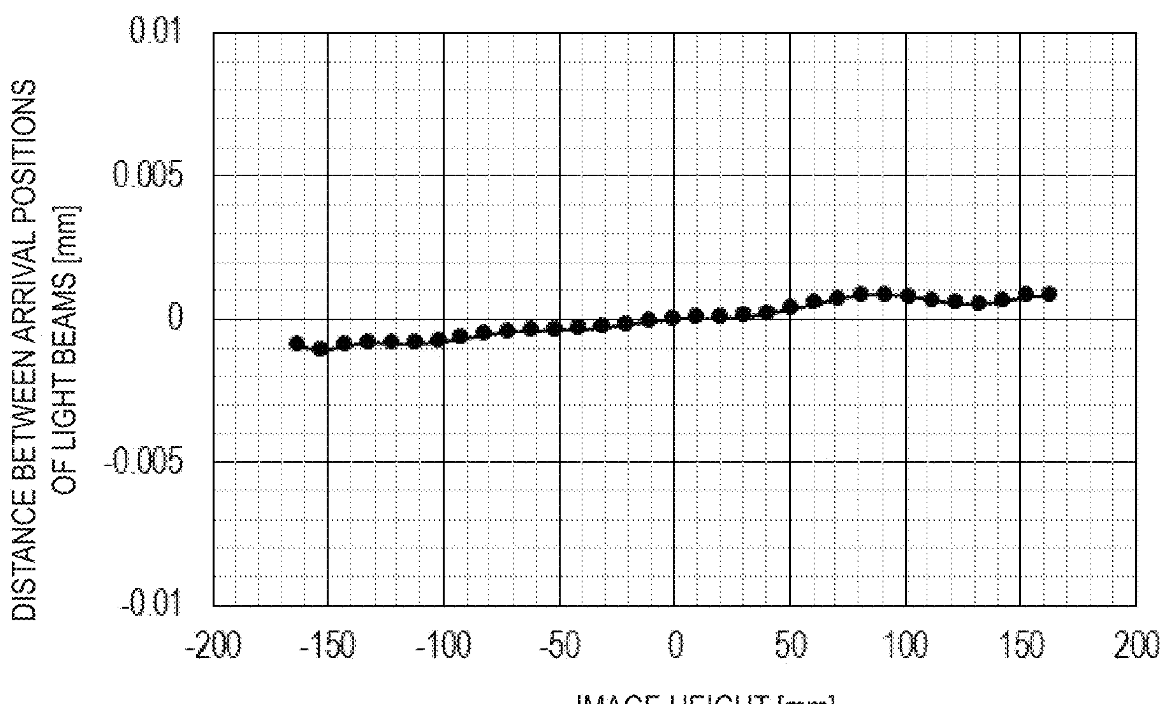

FIG. 13

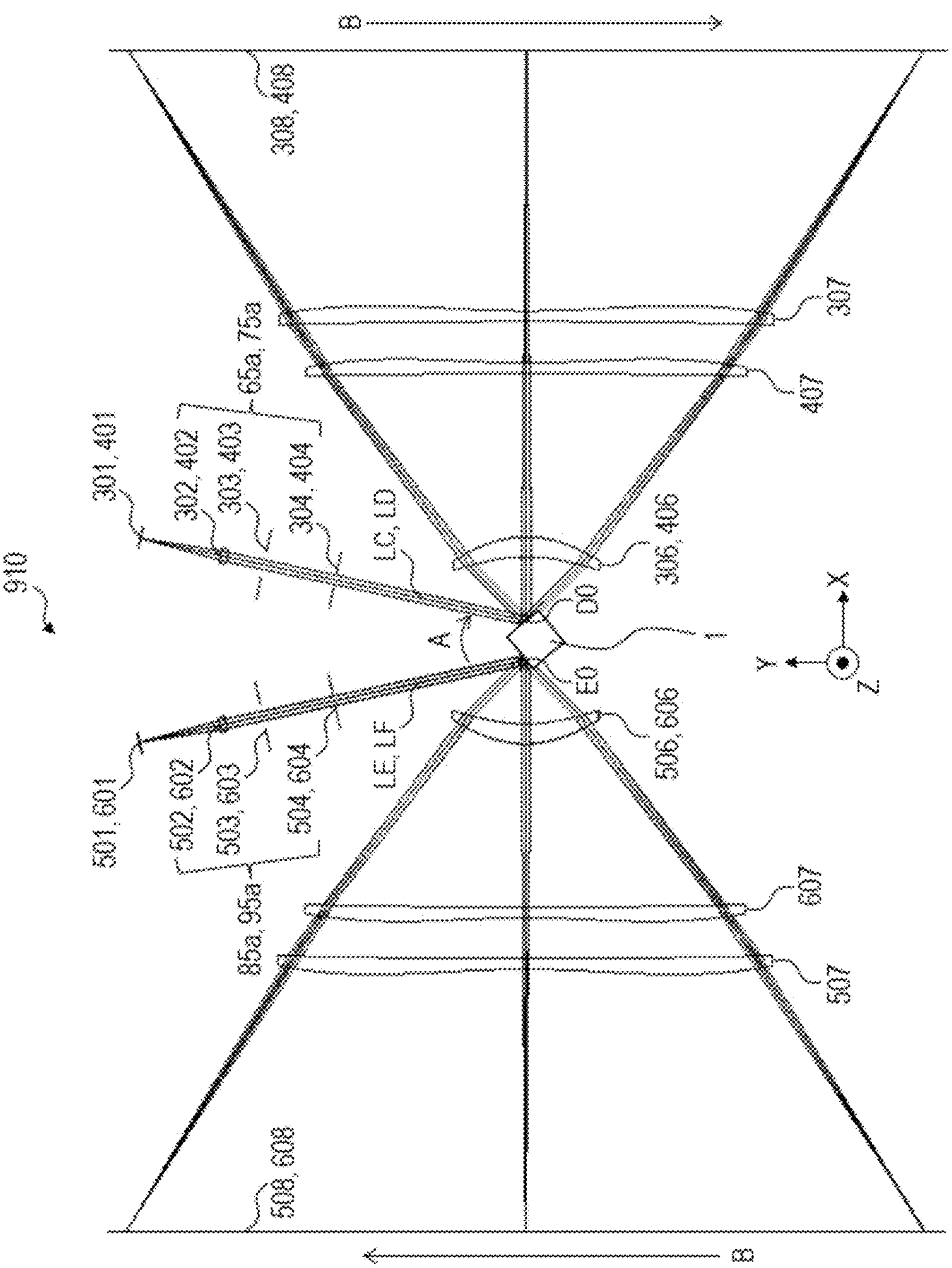
910
B
308, 408
65a, 75a
301, 401
302, 402
303, 403
304, 404
LC, LD
306, 406
307
407
A
D0
E0
1
X
Y
Z
501, 601
502, 602
503, 603
504, 604
LE, LF
506, 606
85a, 95a
607
507
508, 608
B

FIG. 14

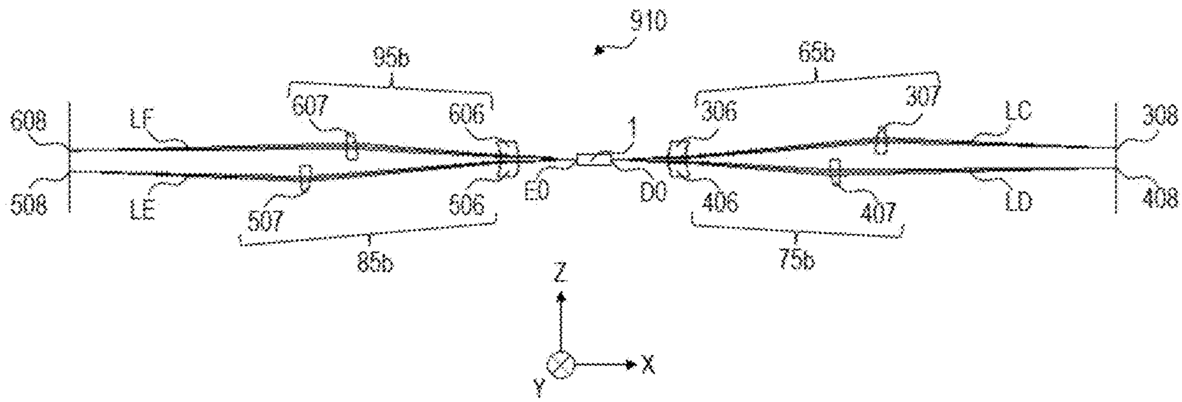
910
95b
65b
608
LF
607
606
1
306
307
LC
308
508
LE
507
506
E0
D0
406
407
LD
408
85b
75b
Z
X
Y

FIG. 15

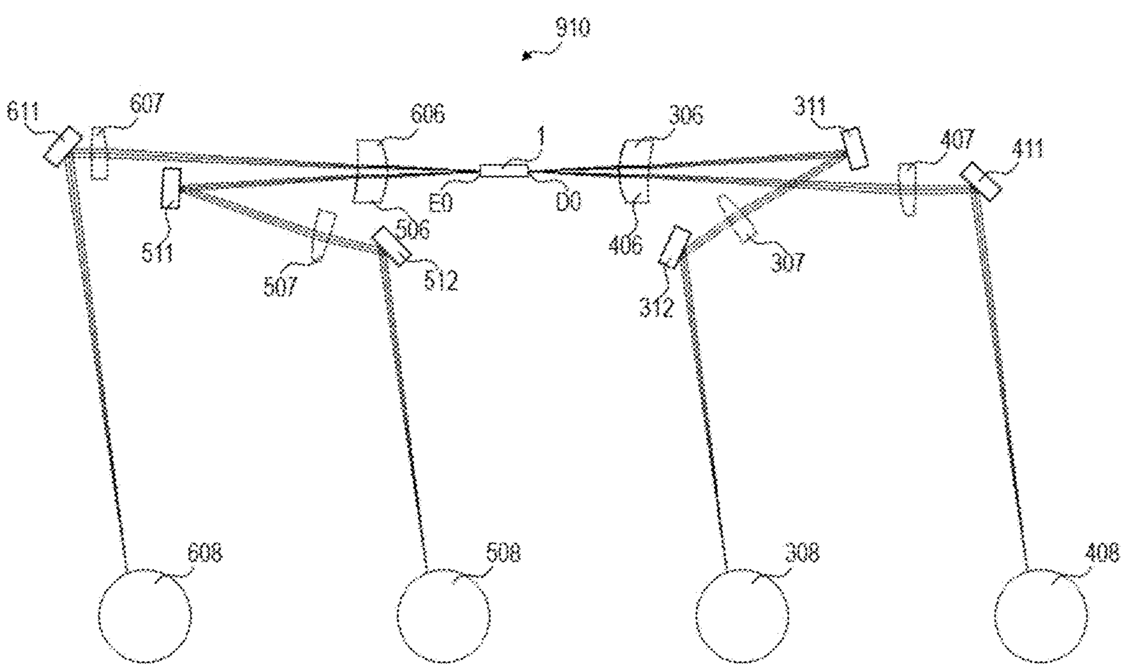
910
611
607
606
1
306
311
407
411
511
E0
506
D0
406
507
512
312
307
608
508
308
408

FIG. 16

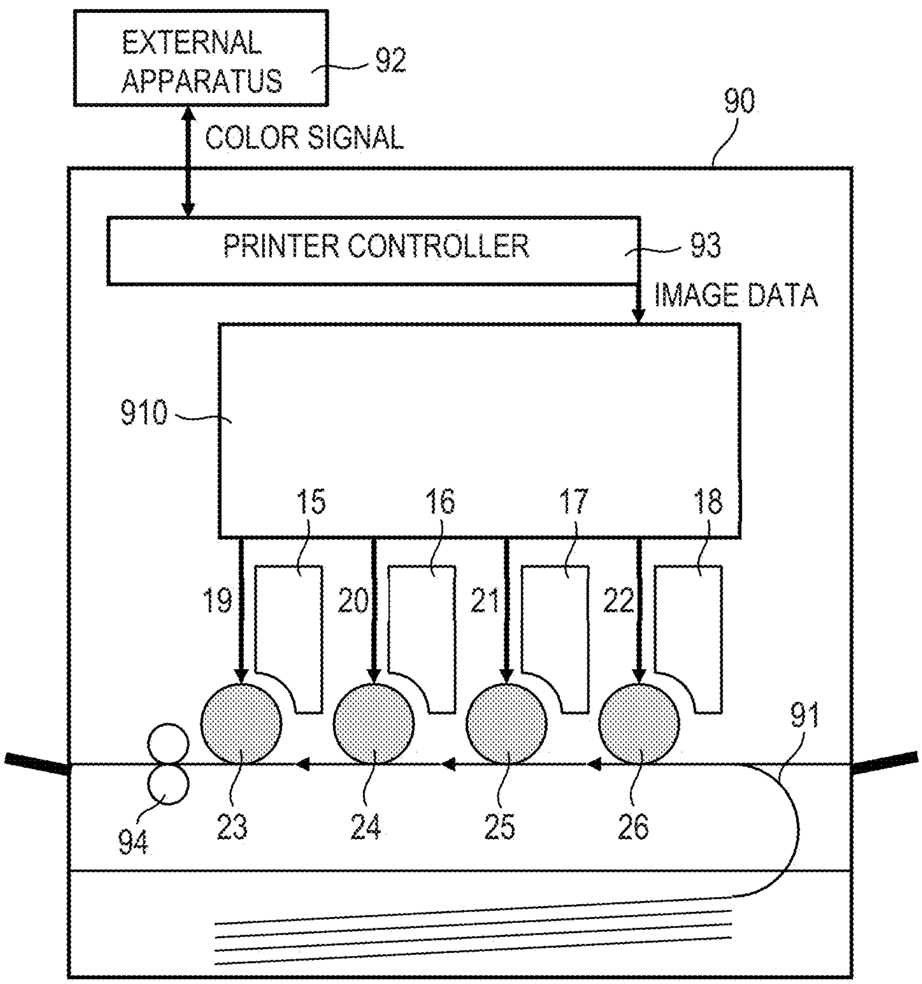
EXTERNAL APPARATUS
92
90
COLOR SIGNAL
PRINTER CONTROLLER
93
IMAGE DATA
910
15
16
17
18
19
20
21
22
91
94
23
24
25
26

LIGHT SCANNING APPARATUS AND IMAGE FORMING APPARATUS

BACKGROUND

Technical Field

[0001] The present disclosure is related to a light scanning apparatus, and more particularly to a light scanning apparatus suitably used in an image forming apparatus such as a laser beam printer (LBP), a digital copying machine and a multi-function printer (MFP).

Description of the Related Art

[0002] Conventionally, there is known a light scanning apparatus which scans a scanned surface by using multiple beams emitted from a light source with a plurality of light emitting points to increase a speed.

[0003] On the other hand, in such light scanning apparatus, it is also known that image quality may deteriorate due to an occurrence of a deviation between scanning widths (overall magnifications) of the multiple beams.

[0004] Japanese Patent Application Laid-open No. H09-197308 discloses a light scanning apparatus that reduces a deviation between scanning widths of multiple beams by using a deviation between scanning widths corresponding to incident angles of the multiple beams with respect to a scanned surface.

SUMMARY

[0005] The apparatus according to the embodiments includes a deflecting unit configured to deflect a plurality of light fluxes from a first light source with a plurality of light emitting points to scan a first scanned surface in a main scanning direction, a first element having a first surface and configured to guide the plurality of light fluxes deflected by a first deflecting surface of the deflecting unit to the first scanned surface, and a first incident system configured to cause the plurality of light fluxes from the first light source to be incident on the first deflecting surface, in which a following condition is satisfied:

$$0.05 < \left| M_{1i}\left[-\beta_1 + \frac{(1-\beta_1)D_1}{L_1} \right] \right| < 0.70,$$

[0006] where L_1 represents a distance between the first light source and the first deflecting surface on an optical axis of the first incident system, D_1 represents a distance between the first deflecting surface and the first surface on an optical axis of the first element, β_1 represents a lateral magnification in a sub-scanning cross section of the first incident system, and M_{1i} represents an inclination of the first surface at a position at which the light flux from an i-th light emitting point of the first light source arrives on the first surface.

[0007] Further features of the disclosure will become apparent from the following description of exemplary embodiments with reference to the attached drawings.

BRIEF DESCRIPTION OF THE DRAWINGS

[0008] FIG. **1**A is a main scanning cross sectional view of a light scanning apparatus according to a first embodiment of the disclosure.

[0009] FIG. **1**B is a partial sub-scanning cross sectional view of the light scanning apparatus according to the first embodiment.

[0010] FIG. **2** is a diagram for explaining an effect in the light scanning apparatus according to the first embodiment.

[0011] FIG. **3**A is a view showing a state in which a plurality of light beams arrive at respective image heights on a scanned surface in the light scanning apparatus according to the first embodiment.

[0012] FIG. **3**B is a view showing a state in which a plurality of light beams arrive at respective image heights on a scanned surface in the light scanning apparatus according to the first embodiment.

[0013] FIG. **4** is a graph showing an image height dependence of a distance between the arrival positions of light beams on the scanned surface in the light scanning apparatus according to the first embodiment.

[0014] FIG. **5**A is a main scanning cross sectional view of a light scanning apparatus according to a second embodiment of the disclosure.

[0015] FIG. **5**B is a partial sub-scanning cross sectional view of the light scanning apparatus according to the second embodiment.

[0016] FIG. **6** is a graph showing an image height dependence of a distance between arrival positions of light beams on a scanned surface in the light scanning apparatus according to the second embodiment.

[0017] FIG. **7**A is a main scanning cross sectional view of a light scanning apparatus according to a third embodiment of the disclosure.

[0018] FIG. **7**B is a partial sub-scanning cross sectional view of the light scanning apparatus according to the third embodiment.

[0019] FIG. **8** is a graph showing an image height dependence of a distance between arrival positions of light beams on a scanned surface in the light scanning apparatus according to the third embodiment.

[0020] FIG. **9**A is a partial developed view in a main scanning cross section of a light scanning apparatus according to a fourth embodiment of the disclosure.

[0021] FIG. **9**B is a partial developed view in the main scanning cross section of the light scanning apparatus according to the fourth embodiment.

[0022] FIG. **10** is a partial developed view in a sub-scanning cross section of the light scanning apparatus according to the fourth embodiment.

[0023] FIG. **11** is a partial sub-scanning cross sectional view of the light scanning apparatus according to the fourth embodiment.

[0024] FIG. **12**A is a graph showing an image height dependence of a distance between arrival positions of light beams on a scanned surface in the light scanning apparatus according to the fourth embodiment.

[0025] FIG. **12**B is a graph showing an image height dependence of a distance between arrival positions of light beams on a scanned surface in the light scanning apparatus according to the fourth embodiment.

[0026] FIG. **13** is a developed view in the main scanning cross section of a light scanning apparatus according to a fifth embodiment of the disclosure.

[0027] FIG. **14** is a partial developed view in the sub-scanning cross section of the light scanning apparatus according to the fifth embodiment.

[0028] FIG. **15** is a partial sub-scanning cross sectional view of the light scanning apparatus according to the fifth embodiment.

[0029] FIG. **16** is a sub-scanning cross sectional view of a main part of an image forming apparatus according to the aspect of the embodiments.

DESCRIPTION OF THE EMBODIMENTS

[0030] Hereinafter, a light scanning apparatus according to the aspect of the embodiments is described in detail with reference to accompanying drawings. Note that the drawings described below may be drawn on a scale different from an actual scale in order to facilitate understanding of the disclosure.

[0031] In the following description, a main scanning direction is a direction perpendicular to a rotation axis of a deflecting unit and an optical axis of an optical system. A sub-scanning direction is a direction parallel to the rotation axis of the deflecting unit. A main scanning cross section is a cross section perpendicular to the sub-scanning direction. The sub-scanning cross section is a cross section perpendicular to the main scanning direction.

[0032] Accordingly, in the following description, it should be noted that the main scanning direction and the sub-scanning cross section are different between an incident optical system and an imaging optical system.

First Embodiment

[0033] FIGS. **1**A and **1**B show a schematic main scanning cross sectional view and a schematic partial sub-scanning cross sectional view of a light scanning apparatus **110** according to a first embodiment of the disclosure, respectively.

[0034] The light scanning apparatus **110** according to the aspect of the embodiment includes a light source **1101** (first light source), an anamorphic collimator lens **1102**, a sub-scanning stop **1103**, a main scanning stop **1104**, a deflecting unit **1**, a first fθ lens **1106** (first optical element, first imaging optical element), and a second fθ lens **1107**.

[0035] On an optical path, the first fθ lens **1106** is arranged between the deflecting unit **1** and the second fθ lens **1107**.

[0036] As the light source **1101**, a semiconductor laser (multibeam laser) or the like having a plurality of light emitting points is used.

[0037] The anamorphic collimator lens **1102** converts a light flux LG emitted from the light source **1101** into a parallel light flux in the main scanning cross section, and condenses the light flux LG in the sub-scanning cross section. The parallel light flux includes not only a strictly parallel light flux but also a substantially parallel light flux such as a weakly divergent light flux or a weakly convergent light flux.

[0038] The sub-scanning stop **1103** limits a light flux diameter in the sub-scanning direction of the light flux LG that has passed through the anamorphic collimator lens **1102**.

[0039] The main scanning stop **1104** limits a light flux diameter in the main scanning direction of the light flux LG that has passed through the sub-scanning stop **1103**.

[0040] With the above-described configuration, the light flux LG emitted from the light source **1101** is condensed in the sub-scanning direction in the vicinity of a deflecting surface of the deflecting unit **1**, so that a line image elongated in the main scanning direction is formed.

[0041] The deflecting unit **1** deflects the incident light flux LG with rotating in a direction indicated by an arrow A in FIG. **1**A by a driving unit such as a motor (not shown). The deflecting unit **1** is formed by a polygon mirror, for example.

[0042] The first fθ lens **1106** and the second fθ lens **1107** are anamorphic imaging lenses having different powers (refractive powers) between the main scanning cross section and the sub-scanning cross section, and condense (guide) the light flux LG deflected by the deflecting unit **1** on the scanned surface **1108** (first scanned surface).

[0043] In the light scanning apparatus **110** according to the aspect of the embodiment, an incident optical system **145**_a_ is formed by the anamorphic collimator lens **1102**, the sub-scanning stop **1103** and the main scanning stop **1104**.

[0044] Further, in the light scanning apparatus **110** according to the aspect of the embodiment, a scanning optical system **145**_b_ (first imaging optical system) is formed by the first fθ lens **1106** and the second fθ lens **1107**.

[0045] Note that the refractive power in the sub-scanning cross section of the second fθ lens **1107** is stronger than the refractive power in the sub-scanning cross section of the first fθ lens **1106**, namely the strongest in the scanning optical system **145**_b_.

[0046] The light fluxes LG emitted from the respective light emitting points of the light source **1101** pass through the incident optical system **145**_a_ to be incident on the deflecting unit **1**.

[0047] The light fluxes LG incident on the deflecting unit **1** from the light source **1101** are deflected by the deflecting unit **1** to be guided onto the scanned surface **1108** by the scanning optical system **145**_b_, thereby the scanned surface **1108** is scanned at a constant speed.

[0048] Since the deflecting unit **1** rotates in the direction indicated by the arrow A in FIG. **1**A, the light fluxes LG deflected by the deflecting unit **1** scan the scanned surface **1108** in a direction indicated by an arrow B in FIG. **1**A.

[0049] In FIGS. **1**A and **1**B, CO represents a deflection point (on-axis deflection point) on the deflecting surface of the deflecting unit **1** for a principal ray of an on-axis light flux. The deflection point CO serves as a reference point of the scanning optical system **145**_b_.

[0050] In the aspect of the embodiment, a photosensitive drum **1108** is used as the scanned surface **1108**. An exposure distribution in the sub-scanning direction on the photosensitive drum **1108** is formed by rotating the photosensitive drum **1108** in the sub-scanning direction for each main scanning exposure.

[0051] Next, various characteristics of the incident optical system **145**_a_ and the scanning optical system **145**_b_ provided in the light scanning apparatus **110** according to the aspect of the embodiment are shown in the following Tables 1 and 2, respectively.

TABLE 1

Characteristics of light source 1101		
Wavelength	λ(nm)	790
Incident polarization to deflecting surface of deflecting unit 1		p-polarization
Full angle at half maximum in main scanning direction	FFPy(deg)	12.00
Full angle at half maximum in sub-scanning direction	FFPz(deg)	30.00

Shape of stop	Main scanning direction	Sub-scanning direction
Sub-scanning stop 1103	10.000	2.840
Main scanning stop 1104	3.750	—

Refractive index	
Anamorphic collimator lens 1102 N1	1.5282

Shape of optical element		Main scanning direction	Sub-scanning direction
Curvature radius of incident surface of anamorphic collimator lens 1102	r1a (mm)	∞	∞
Curvature radius of exit surface of anamorphic collimator lens 1102	r1b (mm)	−37.169	−26.170
Phase coefficient of incident surface	D2, 0	−7.847E−03	—
of anamorphic collimator lens 1102	D0, 2	—	−8.669E−03

Focal length		Main scanning direction	Sub-scanning direction
Anamorphic collimator lens 1102	fcol (mm)	33.94	27.15

Arrangement		
Light source 1101 - Incident surface of anamorphic collimator lens 1102	d0 (mm)	33.59
Incident surface of anamorphic collimator lens 1102 - Exit surface of anamorphic collimator lens 1102	d1 (mm)	3.00
Exit surface of anamorphic collimator lens 1102 - Sub-scanning stop 1103	d2 (mm)	15.15
Sub-scanning stop 1103 - Main scanning stop 1104	d4 (mm)	29.87
Main scanning stop 1104 - Deflecting surface of deflecting unit 1	d5 (mm)	80.09
Incident angle in main scanning cross section of light flux exiting from main scanning stop 1104 to deflecting surface	A1 (deg)	78.00
Incident angle in sub-scanning cross section of light flux exiting from main scanning stop 1104 to deflecting surface	A2 (deg)	−3.00

TABLE 2

fθ coefficient, Scanning width, Maximum angle of view		
fθ coefficient	k (mm/rad)	207
Scanning width	W (mm)	330
Maximum angle of view	θ(deg)	45.7
Refractive index		
Refractive index of first fθ lens 1106	N5	1.5281915
Refractive index of second fθ lens 1107	N6	1.5281915
Deflecting unit 1		
Number of deflecting surfaces		4
Circumscribed radius	Rpol (mm)	10
Rotation center - Deflection reference point C0 (Optical axis direction)	Xpol (mm)	6.03
Rotation center - Deflection reference point C0 (main scanning direction)	Ypol (mm)	3.79
Arrangement in scanning optical system 145b		
Deflection reference point C0 - Incident surface of first fθ lens 1106	d12 (mm)	26.00
Incident surface of first fθ lens 1106 - Exit surface of first fθ lens 1106	d13 (mm)	8.20
Exit surface of first fθ lens 1106 - Incident surface of second fθ lens 1107	d14 (mm)	66.60
Incident surface of second fθ lens 1107 - Exit surface of second fθ lens 1107	d15 (mm)	4.30
Exit surface of second fθ lens 1107 - Scanned surface 1108	d16 (mm)	127.90
Deflection reference point C0 - Incident surface of first f0 lens 1106	L1 (mm)	26.00
Deflection reference point C0 - Incident surface of second fθ lens 1107	L2 (mm)	100.80
Deflection reference point C0 - Scanned surface 1108	T2 (mm)	233.00
Sub-scanning eccentricity of second fθ lens 1107	shiftZ (mm)	−6.99

Meridional line shape of the first fθ lens 1106			Meridional line shape of the first fθ lens 1107		
	Incident surface Opposite light source side	Exit surface Opposite light source side		Incident surface Opposite light source side	Exit surface Opposite light source side
R	−70.147	−42.359	R	−503.226	827.492
ku	8.795E−01	−5.295E−01	ku	0	−6.560E+02
B4u	−2.896E−06	−1.582E−06	B4u	0	−2.864E−07
B6u	8.878E−09	1.735E−09	B6u	0	2.256E−11
B8u	−8.004E−12	1.352E−12	B8u	0	−1.545E−15
B10u	2.358E−15	−1.720E−15	B10u	0	4.648E−20
B12u	0	0	B12u	0	0.000E+00
	Light source side	Light source side		Light source side	Light source side
kl	8.795E−01	−5.295E−01	kl	0	−6.560E+02
B4l	−2.896E−06	1.582E−06	B4l	0	−2.864E−07
B6l	8.878E−09	1.735E−09	B6l	0	2.256E−11
B8l	−8.004E−12	1.352E−12	B8l	0	−1.545E−15
B10l	2.358E−15	−1.720E−15	B10l	0	4.648E−20
B12l	0	0	B12l	0	0.000E+00

Sagittal line shape of first fθ lens 1106			Sagittal line shape of second fθ lens 1107		
	Incident surface Sagittal line R change	Exit surface Sagittal line R change		Incident surface Sagittal line R change	Exit surface Sagittal line R change
r	20.000	41.166	r	54.140	−71.92722
E1	0	0	E1	0.000E+00	−1.809E−06
E2	0	5.090E−05	E2	−1.678E−06	2.363E−07
E3	0	0	E3	0	−1.670E−09
E4	0	−3.069E−08	E4	0.000E+00	−2.510E−10
E5	0	0	E5	0	1.012E−12
E6	0	8.900E−11	E6	0.000E+00	2.098E−14

TABLE 2-continued

E7	0	0	E7	0	−2.168E−16
E8	0	−1.563E−13	E8	0.000E+00	−1.099E−18
E9	0	0	E9	0	1.406E−20
E10	0	9.853E−17	E10	0	3.050E−23
	Sagittal line tilt	Sagittal line tilt		Sagittal line tilt	Sagittal line tilt
M0_1	0	−9.182E−02	M0_1	3.060E−02	1.325E−01
M1_1	0	0	M1_1	−1.540E−05	−3.735E−06
M2_1	0	2.102E−05	M2_1	−2.250E−05	−2.951E−05
M3_1	0	0	M3_1	6.934E−08	5.610E−08
M4_1	0	0	M4_1	5.046E−09	7.008E−09
M5_1	0	0	M5_1	−3.700E−11	−2.746E−11
M6_1	0	0	M6_1	−1.752E−13	−8.318E−13
M7_1	0	0	M7_1	7.276E−15	4.760E−15
M8_1	0	0	M8_1	−4.737E−17	6.909E−17
M9_1	0	0	M9_1	−4.124E−19	−2.153E−19
M10_1	0	0	M10_1	1.935E−21	−5.004E−21
M11_1	0	0	M11_1	0	0
M12_1	0	0	M12_1	0	0

[0052] In Tables 1 and 2, the optical axis, an axis orthogonal to the optical axis in the main scanning cross section, and an axis orthogonal to the optical axis in the sub-scanning cross section are defined as an X-axis, a Y-axis, and a Z-axis, respectively, when an intersection between each lens surface and the optical axis is defined as an origin.

[0053] Further, in Table 2, "E-x" means "$\times 10^{-x}$".

[0054] An aspheric surface shape (meridional line shape) in the main scanning cross section of each lens surface of the first fθ lens **1106** and the second fθ lens **1107** provided in the light scanning apparatus **110** according to the aspect of the embodiment is represented by the following Expression (1):

$$X=\frac{\frac{Y^2}{R}}{1+\sqrt{1-(1+k)\left(\frac{Y}{R}\right)^2}}+\sum_{i=4,6,8,10,12}B_iY^i. \tag{1}$$

[0055] In Expression (1), R represents a curvature radius, k represents an eccentricity, and B_i (i=4, 6, 8, 10 and 12) represent aspheric surface coefficients.

[0056] When the coefficient B_i is different between a positive side and a negative side with respect to Y, a subscript u is added to the coefficient on the positive side (namely, B_{iu}), and a subscript 1 is added to the coefficient on the negative side (namely, B_{i1}), as shown in Table 2.

[0057] An aspheric surface shape (sagittal line shape) in the sub-scanning cross section of each lens surface of the first fθ lens **1106** and the second fθ lens **1107** provided in the light scanning apparatus **110** according to the aspect of the embodiment is represented by the following Expression (2):

$$S=\frac{\frac{Z^2}{r'}}{1+\sqrt{1-\left(\frac{Z}{r'}\right)^2}}+\sum_{j=0}^{12}\sum_{k=1}^{1}M_{jk}Y^jZ^k. \tag{2}$$

[0058] In Expression (2), M_{jk} (j=0 to 12, and k=1) represent aspheric surface coefficients.

[0059] Note that a sagittal line tilt (sagittal line tilt amount) in the aspect of the embodiment indicates the M_{01}. Accordingly, a sagittal line tilt surface refers to a surface whose M_{01} is not 0.

[0060] Further, a curvature radius r' in the sub-scanning cross section of each lens surface of the first fθ lens **1106** and the second fθ lens **1107** provided in the light scanning apparatus **110** according to the aspect of the embodiment continuously varies in accordance with a position in the Y direction as represented by the following Expression (3):

$$r'=\frac{1}{\frac{1}{r}+\sum_{i=1}^{10}E_iY^i}. \tag{3}$$

[0061] In Expression (3), r represents the curvature radius on the optical axis, and E_i (i=1 to 10) represent change coefficients.

[0062] Furthermore, the anamorphic collimator lens **1102** provided in the light scanning apparatus **110** according to the aspect of the embodiment has an incident surface formed by a diffracting surface defined by an optical path difference function of two variables Y and Z as represented by the following expression (4):

$$\varphi(Y,Z)=\frac{2\pi}{\lambda}\sum_{i=0,j=0}D_{ij}Y^iZ^j. \tag{4}$$

[0063] In Expression (4), λ represents a pitch of a diffraction grating, and D_{ij} represent phase coefficients.

[0064] Next, effects of the light scanning apparatus **110** according to the aspect of the embodiment are described.

[0065] FIG. **2** shows a diagram for explaining an effect of the light scanning apparatus **110** according to the aspect of the embodiment.

[0066] In FIG. **2**, light emitting points **2101***a* and **2101***b* that are farthest from a center on opposite sides are shown among the plurality of light emitting points in the light source **1101**.

[0067] Further, in FIG. **2**, an arrow **2102** schematically illustrating the power of the anamorphic collimator lens **1102**, namely the power of the incident optical system **145***a* is shown.

[0068] Furthermore, FIG. **2** shows a position **2103** of the deflecting surface of the deflecting unit **1**, and a combination **2104** of a straight line and a curved line schematically illustrating a shape of the exit surface (first sagittal line tilt surface, first optical surface) of the first fθ lens **1106**, namely the sagittal line tilt coefficient M_{01} and the curvature radius R, respectively.

[0069] FIG. **3**A schematically illustrates a state in which the light beams **2105***a* and **2105***b* emitted from the light emitting points **2101***a* and **2101***b* of the light source **1101** arrive at the positive side outermost off-axis image height, the on-axis image height, and the negative side outermost off-axis image height on the scanned surface **1108** when $\Delta x/d=0$.

[0070] FIG. **3**B schematically illustrates a state in which the light beams **2105***a* and **2105***b* emitted from the light emitting points **2101***a* and **2101***b* of the light source **1101** arrive at the positive side outermost off-axis image height, the on-axis image height, and the negative side outermost off-axis image height on the scanned surface **1108** when $\Delta x/d \neq 0$.

[0071] Here, Δx (mm) represents a distance in a direction parallel to the optical axis between the arrival positions of the light beams **2105***a* and **2105***b* on the exit surface of the first fθ lens **1106**, and d (mm) represents an interval in the sub-scanning direction between the light emitting point **2101***a* and the light emitting point **2101***b*.

[0072] Further, d1, d2 and d3 represent distances in the main scanning direction between the arrival positions of the light beam **2105***a* and **2105***b* at the positive side outermost off-axis image height, the on-axis image height, and the negative side outermost off-axis image height on the scanned surface **1108**, respectively, when Δx/d is 0.

[0073] Furthermore, d4, d5, and d6 represent distances in the main scanning direction between the arrival positions of the light beam **2105***a* and **2105***b* at the positive side outermost off-axis image height, the on-axis image height, and the negative side outermost off-axis image height on the scanned surface **1108**, respectively, when Δx/d is not 0.

[0074] As shown in FIG. **3**A, when Δx/d is 0, a relationship of d1=d2=d3 is satisfied, namely a width of an image formed by the light beam **2105***a* and that of an image formed by the light beam **2105***b* on the scanned surface **1108** are equal to each other.

[0075] On the other hand, when Δx/d is not 0, a relationship of d4≠d5≠d6 is satisfied, namely a width of an image formed by the light beam **2105***a* and that of the image formed by the light beam **2105***b* on the scanned surface **1108** are different from each other.

[0076] In particular, when Δx/d is larger than 0, a relationship of d4>d5>d6 is satisfied as shown in FIG. **3**B, namely a width of an image formed by the light beam **2105***a* is wider than that of the image formed by the light beam **2105***b* on the scanned surface **1108**.

[0077] Here, a distance on the optical axis between the light source **1101** and the deflecting surface of the deflecting unit **1** is represented by L (mm), and a distance in the sub-scanning direction between a center of the light source **1101** and the light emitting point **2101***a* or the light emitting point **2101***b* is represented by d_0 (mm). That is, a relationship of $d_0=d/2$ is satisfied.

[0078] The position of the light source **1101** on the optical axis can be obtained as an intersection between a plane including the plurality of light emitting points provided in the light source **1101** and the optical axis.

[0079] Further, an angle formed by a straight line passing through the light emitting point **2101***a* or the light emitting point **2101***b*, and the center of the anamorphic collimator lens **1102** with respect to the optical axis in the sub-scanning cross section is represented by θ (degrees).

[0080] A lateral magnification of the anamorphic collimator lens **1102** in the sub-scanning cross section, namely the lateral magnification of the incident optical system **145***a* in the sub-scanning cross section is represented by β.

[0081] At this time, a height in the sub-scanning direction of the arrival position of the light beam **2105***a* or the light beam **2105***b* on the deflecting surface of the deflecting unit **1** is represented by $-\beta \times d_0$, so that the following Expression (5) is obtained:

$$\tan\theta = \frac{(1-\beta)d_0}{L}. \tag{5}$$

[0082] Next, the curvature radius in the sub-scanning cross section of the exit surface of the first fθ lens **1106** on the optical axis is represented by R (mm), and an eccentricity amount in the sub-scanning direction of the first fθ lens **1106** is represented by L_s (mm).

[0083] At this time, an inclination M at the arrival position of the light beam **2105***a* or the light beam **2105***b* on the exit surface of the first fθ lens **1106** can be approximately expressed by the following Expression (6) using the aspheric surface coefficient M_{01} shown in the Expression (2) corresponding to the sagittal line tilt amount on the optical axis:

$$M = \frac{L_s}{R} + M_{01}. \tag{6}$$

[0084] The inclination M of the exit surface of the first fθ lens **1106** is defined as an inclination of a normal of the exit surface of the first fθ lens **1106** with respect to the optical axis.

[0085] Further, when a distance in the sub-scanning direction between the arrival positions of the light beam **2105***a* and the light beam **2105***b* on the exit surface of the first fθ lens **1106** is represented by Δy (mm), the following Expression (7) is obtained:

$$\Delta x = M \times \Delta y. \tag{7}$$

[0086] When a distance on the optical axis between the deflecting surface of the deflecting unit **1** and the exit surface of the first fθ lens **1106** is represented by D (mm), Δy can be expressed by the following Expression (8):

$$\Delta y = 2(-\beta d_0 + D\tan\theta) = 2d_0\left[-\beta + \frac{(1-\beta)D}{L}\right]. \tag{8}$$

[0087] Note that Expression (5) is used when Expression (8) is derived.

[0088] Accordingly, Δx/d can be expressed by the following Expression (9) using Expressions (7) and (8):

$$\frac{\Delta x}{d} = \frac{M\times\Delta y}{2d_0} = M\left[-\beta + \frac{(1-\beta)D}{L}\right]. \tag{9}$$

[0089] Further, Equation (9) can be rewritten as the following Expression (10) by using Expression (6):

$$\frac{\Delta x}{d} = \left[\frac{L_s}{R} + M_{01}\right]\times\left[-\beta + \frac{(1-\beta)D}{L}\right]. \tag{10}$$

[0090] When a value of Δx/d is small, a difference between an inclination of a light beam incident on the first fθ lens **1106** and an inclination of the light beam exiting from the first fθ lens **1106** becomes small.

[0091] Therefore, a degree of freedom in an arrangement of the second fθ lens **1107** and the photosensitive drum **1108** is reduced, so that it is difficult to sufficiently reduce the size.

[0092] On the other hand, when the value of Δx/d is large, the light beams **2105***a* and **2105***b* emitted from the light emitting points **2101***a* and **2101***b* pass through such first fθ lens **1106**, and thus the difference between the widths of the images formed by the light beams **2105***a* and **2105***b* becomes large as described above with reference to FIG. **3**B.

[0093] Accordingly, in the light scanning apparatus **110** according to the aspect of the embodiment, both of downsizing and high definition be achieved by satisfying the following Inequality (11) for an absolute value of Δx/d.

[0094] In other words, in the light scanning apparatus **110** according to the aspect of the embodiment, the following Inequality (11) be satisfied for all of the light emitting points of the light source **1101**:

$$0.05 < \left|M\left[-\beta + \frac{(1-\beta)D}{L}\right]\right| < 0.70. \tag{11}$$

[0095] In the light scanning apparatus **110** according to the aspect of the embodiment, the following Inequality (11a) be satisfied instead of Inequality (11) for all of the light emitting points of the light sources **1101**:

$$0.10 < \left|M\left[-\beta + \frac{(1-\beta)D}{L}\right]\right| < 0.65. \tag{11a}$$

[0096] Further, in the light scanning apparatus **110** according to the aspect of the embodiment, the following Inequality (11b) be satisfied instead of Inequality (11a) for all the light emitting points of the light sources **1101**:

$$0.15 < \left|M\left[-\beta + \frac{(1-\beta)D}{L}\right]\right| < 0.60. \tag{11b}$$

[0097] Note that the above-described effect can be obtained when Inequalities (11), (11a) and (11b) are satisfied for at least one of the light emitting points of the light sources **1101** although Inequalities (11), (11a) and (11b) are satisfied for all the light emitting points of the light sources **1101**.

[0098] In addition, as an inclination amount of the exit surface of the first fθ lens **1106**, namely the sagittal line tilt coefficient M_{01} increases, the difference between the widths of the images formed by the light beams **2105***a* and **2105***b* increases.

[0099] Therefore, in the light scanning apparatus **110** according to the aspect of the embodiment, the following Inequality (12) be satisfied:

$$0 < \left|M_{01}\left[-\beta + \frac{(1-\beta)D}{L}\right]\right| < 0.185. \tag{12}$$

[0100] In addition, when the exit surface of the first fθ lens **1106** has a curvature, the inclination amounts at the arrival positions on the exit surface of the light beams emitted from the respective light emitting points of the light source **1101** is different from each other.

[0101] Therefore, in the light scanning apparatus **110** according to the aspect of the embodiment, the following Inequality (13) be satisfied:

$$0.05 < \left|\left[\frac{L_s}{R} + M_{01}\right]\times\left[-\beta + \frac{(1-\beta)D}{L}\right]\right| < 0.70. \tag{13}$$

[0102] Specifically, β is −3.65, D is 34.2 mm, Lis 161.7 mm, and M is −0.127 in the light scanning apparatus **110** according to the aspect of the embodiment.

[0103] Accordingly, the value of each of Inequalities (11), (11a) and (11b) is calculated as 0.589, so that Inequalities (11), (11a) and (11b) are satisfied.

[0104] On the other hand, in the light scanning apparatus **110** according to the aspect of the embodiment, since M_{01} is −0.0918, the value of Inequality (12) is calculated as 0.426, so that Inequality (12) is not satisfied.

[0105] Further, in the light scanning apparatus **110** according to the aspect of the embodiment, since L_s is −1.45 mm and R is 41.166 mm, the value of Inequality (13) is calculated as 0.589, so that Inequality (13) is satisfied.

[0106] The sagittal line tilt amount of the exit surface of the first fθ lens **1106** provided in the light scanning apparatus **110** according to the aspect of the embodiment varies according to the position in the main scanning direction.

[0107] Then, an absolute value of the sagittal line tilt amount of the exit surface of the first fθ lens **1106** is the largest on the optical axis.

[0108] Further, the first fθ lens **1106** has a positive power in the sub-scanning cross section.

[0109] Further, the first fθ lens **1106** closest to the deflecting unit **1** on the optical path of the light flux LG among the fθ lenses included in the scanning optical system **145***b*, is an fθ lens having the strongest power in the main scanning cross section among the fθ lenses included in the scanning optical system **145***b*.

[0110] FIG. **4** shows distances in the main scanning direction between the arrival positions of the light beams **2105***a* and **2105***b* at respective image heights on the scanned surface **1108** in the light scanning apparatus **110** according to the aspect of the embodiment.

[0111] That is, the distances include d4, d5 and d6 shown in FIG. **3**B, and the distance at the on-axis image height is shown as 0 mm in FIG. **4**.

[0112] As shown in FIG. **4**, in the light scanning apparatus **110** according to the aspect of the embodiment, a difference between a maximum value and a minimum value of the distances is 8.0 μm.

[0113] Since the difference corresponds to a deviation of about 9.4% with respect to 300 dpi, namely a pitch of 84.7 μm, an influence of the deviation of the arrival position of each light beam on the scanned surface **1108** on the image quality can be reduced.

[0114] As described above, in the light scanning apparatus **110** according to the aspect of the embodiment, it is possible to suppress a deterioration of the image quality due to the deviation of the arrival position of each light beam on the scanned surface **1108** by satisfying Inequality (11).

[0115] In addition, in the light scanning apparatus **110** according to the aspect of the embodiment, it is possible to achieve downsizing by forming the exit surface of the first fθ lens **1106** as a sagittal line tilt surface.

Second Embodiment

[0116] FIGS. **5**A and **5**B show a schematic main scanning cross sectional view and a schematic partial sub-scanning cross sectional view of a light scanning apparatus **310** according to a second embodiment of the disclosure, respectively.

[0117] The light scanning apparatus **310** according to the aspect of the embodiment has the same configuration as the light scanning apparatus **110** according to the first embodiment except that the specification values are different, so that the same members are denoted by the same reference numerals, and description thereof is omitted.

[0118] Specifically, various characteristics of the incident optical system **145***a* and the scanning optical system **145***b* provided in the light scanning apparatus **310** according to the aspect of the embodiment are shown in the following Tables 3 and 4, respectively.

TABLE 3

Characteristics of light source 1101		
Wavelength	λ(nm)	790
Incident polarization to deflecting surface of deflecting unit 1		p polarization
Full angle at half maximum in main scanning direction	FFPy(deg)	12.00
Full angle at half maximum in sub-scanning direction	FFPz(deg)	30.00

Shape of stop	Main scanning direction	Sub-scanning direction
Sub-scanning stop 1103	10.000	2.840
Main scanning stop 1104	3.750	—

Refractive index		
Anamorphic collimator lens 1102	N1	1.5282

Shape of optical element		Main scanning direction	Sub-scanning direction
Curvature radius of incident surface of anamorphic collimator lens 1102	r1a (mm)	∞	∞
Curvature radius of exit surface of anamorphic collimator lens 1102	r1b (mm)	−37.169	−26.170
Phase coefficient of incident surface of anamorphic collimator lens 1102	D2, 0	−7.847E−03	—
	D0, 2	—	−8.669E−03

TABLE 3-continued

Focal length			
		Main scanning direction	Sub-scanning direction
Anamorphic collimator lens 1102	fcol (mm)	33.94	27.15

Arrangement		
Light source 1101 - Incident surface of anamorphic collimator lens 1102	d0 (mm)	33.59
Incident surface of anamorphic collimator lens 1102 - Exit surface of anamorphic collimator lens 1102	d1 (mm)	3.00
Exit surface of anamorphic collimator lens 1102 - Sub-scanning stop 1103	d2 (mm)	15.15
Sub-scanning stop 1103 - Main scanning stop 1104	d4 (mm)	29.87
Main scanning stop 1104 - Deflecting surface of deflecting unit 1	d5 (mm)	80.09
Incident angle in main scanning cross section of light flux exiting from main scanning stop 1104 to deflecting surface	A1 (deg)	78.00
Incident angle in sub-scanning cross section of light flux exiting from main scanning stop 1104 to deflecting surface	A2 (deg)	−3.00

TABLE 4

fθ coefficient, Scanning width, Maximum angle of view		
fθ coefficient	k (mm/rad)	207
Scanning width	W (mm)	330
Maximum angle of view	θ(deg)	45.7
Refractive index		
Refractive index of first fθ lens 1106	N5	1.5281915
Refractive index of second fθ lens 1107	N6	1.5281915
Deflecting unit 1		
Number of deflecting surfaces		4
Circumscribed radius	Rpol (mm)	10
Rotation center - Deflection reference point C0 (Optical axis direction)	Xpol (mm)	6.03
Rotation center - Deflection reference point C0 (main scanning direction)	Ypol (mm)	3.79
Arrangement in scanning optical system 145b		
Deflection reference point C0 - Incident surface of first fθ lens 1106	d12 (mm)	26.00
Incident surface of first fθ lens 1106 - Exit surface of first fθ lens 1106	d13 (mm)	8.20
Exit surface of first fθ lens 1106 - Incident surface of second fθ lens 1107	d14 (mm)	66.60
Incident surface of second fθ lens 1107 - Exit surface of second fθ lens 1107	d15 (mm)	4.30
Exit surface of second fθ lens 1107 - Scanned surface 1108	d16 (mm)	127.90
Deflection reference point C0 - Incident surface of first fθ lens 1106	L1 (mm)	26.00
Deflection reference point C0 - Incident surface of second fθ lens 1107	L2 (mm)	100.80

TABLE 4-continued

Deflection reference point C0 - Scanned surface 1108		T2 (mm)	233.00
Sub-scanning eccentricity of second fθ lens 1107		shiftZ (mm)	−1.37

Meridional line shape of first fθ lens 1106			Meridional line shape of first fθ lens 1107		
	Incident surface Opposite light source side	Exit surface Opposite light source side		Incident surface Opposite light source side	Exit surface Opposite light source side
R	−66.242	−40.841	R	−494.7832	802.295
ku	8.020E−01	−5.277E−01	ku	0	−6.789E+02
B4u	−2.796E−06	−1.602E−06	B4u	0	−2.895E−07
B6u	8.876E−09	1.735E−09	B6u	0	2.255E−11
B8u	−7.979E−12	1.355E−12	B8u	0	−1.522E−15
B10u	2.370E−15	−1.715E−15	B10u	0	4.450E−20
B12u	0	0	B12u	0	0.000E+00
	Light source side	Light source side		Light source side	Light source side
k1	8.020E−01	−5.277E−01	k1	0	−6.789E+02
B41	−2.796E−06	−1.602E−06	B41	0	−2.895E−07
B61	8.876E−09	1.735E−09	B61	0	2.255E−11
B81	−7.979E−12	1.355E−12	B81	0	−1.522E−15
B101	2.370E−15	−1.715E−15	B101	0	4.450E−20
B121	0	0	B121	0	0.000E+00

Sagittal line shape of first fθ lens 1106			Sagittal line shape of first fθ lens 1107		
	Incident surface Sagittal line R change	Exit surface Sagittal line R change		Incident surface Sagittal line R change	Exit surface Sagittal line R change
r	50.000	76.858	r	46.640	−79.14512
E1	0	0	E1	0.000E+00	−1.460E−06
E2	0	2.018E−05	E2	−1.990E−06	3.054E−07
E3	0	0	E3	0	−1.037E−09
E4	0	−1.126E−08	E4	0.000E+00	−2.859E−10
E5	0	0	E5	0	7.163E−13
E6	0	6.930E−11	E6	0.000E+00	1.866E−14
E7	0	0	E7	0	−1.675E−16
E8	0	−2.386E−14	E8	0.000E+00	−1.281E−19
E9	0	0	E9	0	1.2395E−20
E10	0	−7.962E−17	E10	0	−4.877E−23
	Sagittal line tilt	Sagittal line tilt		Sagittal line tilt	Sagittal line tilt
M0_1	0	−3.850E−02	M0_1	8.966E−02	7.878E−02
M1_1	0	0	M1_1	−3.516E−06	−2.624E−06
M2_1	0	−4.057E−05	M2_1	−2.739E−05	−2.545E−05
M3_1	0	0	M3_1	6.075E−08	5.025E−08
M4_1	0	0	M4_1	5.534E−09	6.347E−09
M5_1	0	0	M5_1	−3.749E−11	−2.803E−11
M6_1	0	0	M6_1	−2.101E−13	−8.019E−13
M7_1	0	0	M7_1	7.252E−15	4.725E−15
M8_1	0	0	M8_1	−5.256E−17	7.298E−17
M9_1	0	0	M9_1	−4.108E−19	−2.157E−19
M10_1	0	0	M10_1	2.174E−21	−5.879E−21
M11_1	0	0	M11_1	0	0
M12_1	0	0	M12_1	0	0

[0119] In Tables 3 and 4, an optical axis, an axis orthogonal to the optical axis in the main scanning cross section, and an axis orthogonal to the optical axis in the sub-scanning cross section are defined as an X-axis, a Y-axis, and a Z-axis, respectively, when an intersection between each lens surface and the optical axis is defined as an origin.

[0120] Further, in Table 4, "E-x" means "$\times 10^{-x}$".

[0121] An aspheric surface shape (meridional line shape) in the main scanning cross section of each lens surface of the first fθ lens **1106** and the second fθ lens **1107** provided in the light scanning apparatus **310** according to the aspect of the embodiment is represented by the above-described Expression (1).

[0122] An aspheric surface shape (sagittal line shape) in the sub-scanning cross section of each lens surface of the first fθ lens **1106** and the second fθ lens **1107** provided in the light scanning apparatus **310** according to the aspect of the embodiment is represented by the above-described Expression (2).

[0123] A curvature radius r' in the sub-scanning cross section of each lens surface of the first fθ lens **1106** and the second fθ lens **1107** provided in the light scanning apparatus **310** according to the aspect of the embodiment continuously varies in accordance with a position in the Y direction as represented by the above-described Expression (3).

[0124] The anamorphic collimator lens **1102** provided in the light scanning apparatus **310** according to the aspect of the embodiment has an incident surface formed by a diffracting surface defined by the optical path difference function of two variables Y and Z as represented by the above-described Expression (4).

[0125] Further, in the light scanning apparatus **310** according to the aspect of the embodiment, Inequality (11) be satisfied, Inequality (11a) be satisfied, and Inequality (11b) be satisfied.

[0126] In the light scanning apparatus **310** according to the aspect of the embodiment, Inequalities (12) and (13) be satisfied.

[0127] Specifically, in the light scanning apparatus **310** according to the aspect of the embodiment, β is −3.65, D is 34.2 mm, Lis 161.7 mm, and M is −0.0385.

[0128] Therefore, a value of each of Inequalities (11), (11a) and (11b) is calculated as 0.179, so that Inequalities (11), (11a) and (11b) are satisfied.

[0129] Further, in the light scanning apparatus **310** according to the aspect of the embodiment, since M_{01} is −0.0385, a value of Inequality (12) is calculated as 0.179, so that Inequality (12) is satisfied.

[0130] Furthermore, in the light scanning apparatus **310** according to the aspect of the embodiment, since L_s is 0 mm and R is 76.858 mm, a value of Inequality (13) is calculated as 0.179, so that Inequality (13) is satisfied.

[0131] FIG. **6** shows distances in the main scanning direction between arrival positions of light beams **2105*a*** and **2105*b*** at respective image heights on the scanned surface **1108** in the light scanning apparatus **310** according to the aspect of the embodiment.

[0132] That is, the distances include d4, d5, and d6 shown in FIG. **3**B, and the distance at the on-axis image height is shown as 0 mm in FIG. **6**.

[0133] As shown in FIG. **6**, in the light scanning apparatus **310** according to the aspect of the embodiment, a difference between a maximum value and a minimum value of the distances is 5.9 μm.

[0134] Since the difference corresponds to a deviation of about 7.0% with respect to 300 dpi, namely a pitch of 84.7 μm, an influence of the deviation of the arrival position of each light beam on the scanned surface **1108** on the image quality can be reduced. As described above, in the light scanning apparatus **310** according to the aspect of the embodiment, it is possible to suppress a deterioration of the image quality due to the deviation of the arrival position of each light beam on the scanned surface **1108** by satisfying Inequality (11).

Third Embodiment

[0135] FIGS. **7**A and **7**B show a schematic main scanning cross sectional view and a schematic partial sub-scanning cross sectional view of a light scanning apparatus **510** according to a third embodiment of the disclosure, respectively.

[0136] The light scanning apparatus **510** according to the aspect of the embodiment has the same configuration as the light scanning apparatus **110** according to the first embodiment except that the specification values are different, so that the same members are denoted by the same reference numerals, and description thereof is omitted.

[0137] Specifically, various characteristics of the incident optical system **145*a*** and the scanning optical system **145*b*** provided in the light scanning apparatus **510** according to the aspect of the embodiment are shown in the following Tables 5 and 6, respectively.

TABLE 5

Characteristics of light source 1101		
Wavelength	λ(nm)	790
Incident polarization to deflecting surface of deflecting unit 1		p polarization
Full angle at half maximum in main scanning direction	FFPy(deg)	12.00
Full angle at half maximum in sub-scanning direction	FFPz(deg)	30.00

Shape of stop	Main scanning direction	Sub-scanning direction
Sub-scanning stop 1103	10.000	2.840
Main scanning stop 1104	3.750	—

Refractive index		
Anamorphic collimator lens 1102	N1	1.5282

Shape of optical element		Main scanning direction	Sub-scanning direction
Curvature radius of incident surface of anamorphic collimator lens 1102	r1a (mm)	∞	∞
Curvature radius of exit surface of anamorphic collimator lens 1102	r1b (mm)	−37.169	−26.170
Phase coefficient of incident surface	D2, 0	−7.847E-03	—
of anamorphic collimator lens 1102	D0, 2	—	−8.669E-03

Focal length		Main scanning direction	Sub-scanning direction
Anamorphic collimator lens 1102	fcol (mm)	33.94	27.15

Arrangement		
Light source 1101 - Incident surface of anamorphic collimator lens 1102	d0 (mm)	33.59
Incident surface of anamorphic collimator lens 1102 - Exit surface of anamorphic collimator lens 1102	d1 (mm)	3.00
Exit surface of anamorphic collimator lens 1102 - Sub-scanning stop 1103	d2 (mm)	15.15
Sub-scanning stop 1103 - Main scanning stop 1104	d4 (mm)	29.87
Main scanning stop 1104 - Deflecting surface of deflecting unit 1	d5 (mm)	80.09
Incident angle in main scanning cross section of light flux exiting from main scanning stop 1104 to deflecting surface	A1 (deg)	78.00
Incident angle in sub-scanning cross section of light flux exiting from main scanning stop 1104 to deflecting surface	A2 (deg)	−3.00

TABLE 6

fθ coefficient, Scanning width, Maximum angle of view		
fθ coefficient	k (mm/rad)	207
Scanning width	W (mm)	330
Maximum angle of view	θ(deg)	45.7
Refractive index		
Refractive index of first fθ lens 1106	N5	1.5281915
Refractive index of second fθ lens 1107	N6	1.5281915
Deflecting unit 1		
Number of deflecting surfaces		4
Circumscribed radius	Rpol (mm)	10
Rotation center - Deflection reference point C0 (Optical axis direction)	Xpol (mm)	6.03
Rotation center - Deflection reference point C0 (main scanning direction)	Ypol (mm)	3.79
Arrangement in scanning optical system 145b		
Deflection reference point C0 - Incident surface of first fθ lens 1106	d12 (mm)	26.00
Incident surface of first fθ lens 1106 - Exit surface of first fθ lens 1106	d13 (mm)	8.20
Exit surface of first fθ lens 1106 - Incident surface of second fθ lens 1107	d14 (mm)	69.30
Incident surface of second fθ lens 1107 - Exit surface of second fθ lens 1107	d15 (mm)	4.30
Exit surface of second fθ lens 1107 - Scanned surface 1108	d16 (mm)	125.20
Deflection reference point C0 - Incident surface of first fθ lens 1106	L1 (mm)	26.00
Deflection reference point C0 - Incident surface of second fθ lens 1107	L2 (mm)	103.50
Deflection reference point C0 - Scanned surface 1108	T2 (mm)	233.00
Sub-scanning eccentricity of second fθ lens 1107	shiftZ (mm)	−5.03

	Meridional line shape of first fθ lens 1106			Meridional line shape of first fθ lens 1107	
	Incident surface Opposite light source side	Exit surface Opposite light source side		Incident surface Opposite light source side	Exit surface Opposite light source side
R	−71.101	−42.946	R	−4000	350.123
ku	9.464E−01	−5.155E−01	ku	0	−8.753E+01
B4u	−9.147E−07	−3.477E−07	B4u	0	−2.020E−07
B6u	6.784E−09	1.690E−09	B6u	0	1.609E−11
B8u	−5.767E−12	1.110E−12	B8u	0	−9.313E−16
B10u	1.638E−15	−1.224E−15	B10u	0	2.524E−20
B12u	0	0	B12u	0	0.000E+00
	Light source side	Light source side		Light source side	Light source side
k1	9.464E−01	−5.155E−01	k1	0	−8.753E+01
B41	−9.147E−07	−3.477E−07	B41	0	−2.020E−07
B61	6.784E−09	1.690E−09	B61	0	1.609E−11

TABLE 6-continued

B81	−5.767E−12	1.110E−12	B81	0	−9.313E−16
B101	1.638E−15	−1.224E−15	B101	0	2.524E−20
B121	0	0	B121	0	0.000E+00

	Sagittal line shape of first fθ lens 1106			Sagittal line shape of second fθ lens 1107	
	Incident surface Sagittal line R change	Exit surface Sagittal line R change		Incident surface Sagittal line R change	Exit surface Sagittal line R change
r	20.000	25.004	r	37.079	−154.0078
E1	0	0	E1	0.000E+00	−1.278E−07
E2	0	1.522E−05	E2	−7.458E−07	1.813E−06
E3	0	0	E3	0	−3.240E−09
E4	0	8.486E−10	E4	0.000E+00	−3.041E−10
E5	0	0	E5	0	1.339E−12
E6	0	−2.508E−11	E6	0.000E+00	3.082E−14
E7	0	0	E7	0	−2.009E−16
E8	0	7.607E−15	E8	0.000E+00	−1.954E−18
E9	0	0	E9	0	9.85865E−21
E10	0	1.610E−17	E10	0	5.812E−23
	Sagittal line tilt	Sagittal line tilt		Sagittal line tilt	Sagittal line tilt
M0_1	0	−2.124E−02	M0_1	−1.007E−01	2.315E−02
M1_1	0	0	M1_1	−2.129E−04	−2.002E−04
M2_1	0	3.321E−05	M2_1	−1.314E−05	−2.370E−05
M3_1	0	0	M3_1	1.161E−07	1.056E−07
M4_1	0	0	M4_1	1.765E−09	3.675E−09
M5_1	0	0	M5_1	−1.616E−11	−1.409E−11
M6_1	0	0	M6_1	3.014E−13	−3.052E−13
M7_1	0	0	M7_1	1.061E−15	9.733E−16
M8_1	0	0	M8_1	−1.306E−17	6.574E−17
M9_1	0	0	M9_1	−1.657E−20	−1.728E−20
M10_1	0	0	M10_1	−8.536E−22	−3.960E−21
M11_1	0	0	M11_1	0	0
M12_1	0	0	M12_1	0	0

[0138] In Tables 5 and 6, an optical axis, an axis orthogonal to the optical axis in the main scanning cross section, and an axis orthogonal to the optical axis in the sub-scanning cross section are defined as an X-axis, a Y-axis, and a Z-axis, respectively, when an intersection between each lens surface and the optical axis is defined as an origin.

[0139] Further, in Table 6, "E-x" means "$\times 10^{-x}$".

[0140] An aspheric surface shape (meridional line shape) in the main scanning cross section of each lens surface of the first fθ lens **1106** and the second fθ lens **1107** provided in the light scanning apparatus **510** according to the aspect of the embodiment is represented by the above-described Expression (1).

[0141] An aspheric surface shape (sagittal line shape) in the sub-scanning cross section of each lens surface of the first fθ lens **1106** and the second fθ lens **1107** provided in the light scanning apparatus **510** according to the aspect of the embodiment is represented by the above-described Expression (2).

[0142] A curvature radius r' in the sub-scanning cross section of each lens surface of the first fθ lens **1106** and the second fθ lens **1107** provided in the light scanning apparatus **510** according to the aspect of the embodiment continuously varies in accordance with a position in the Y direction as represented by the above-described Expression (3).

[0143] The anamorphic collimator lens **1102** provided in the light scanning apparatus **510** according to the aspect of the embodiment has an incident surface formed by a diffracting surface defined by the optical path difference function of two variables Y and Z as represented by the above-described Expression (4).

[0144] Further, in the light scanning apparatus **510** according to the aspect of the embodiment, Inequality (11) be satisfied, Inequality (11a) be satisfied, and Inequality (11b) be satisfied.

[0145] In the light scanning apparatus **510** according to the aspect of the embodiment, Inequalities (12) and (13) be satisfied.

[0146] Specifically, in the light scanning apparatus **510** according to the aspect of the embodiment, β is −3.65, D is 34.2 mm, Lis 161.7 mm, and M is −0.0735.

[0147] Therefore, a value of each of Inequalities (11), (11a) and (11b) is calculated as 0.341, and Inequalities (11), (11a) and (11b) are satisfied.

[0148] Further, in the light scanning apparatus **510** according to the aspect of the embodiment, since M_{01} is −0.0212, a value of Inequality (12) is calculated as 0.098, so that Inequality (12) is satisfied.

[0149] Furthermore, in the light scanning apparatus **510** according to the aspect of the embodiment, since L_s is −1.31 mm and R is 25.004 mm, a value of Inequality (13) is calculated as 0.341, so that Inequality (13) is satisfied.

[0150] FIG. **8** shows distances in the main scanning direction between arrival positions of light beams **2105***a* and

2105*b* at respective image heights on the scanned surface **1108** in the light scanning apparatus **510** according to the aspect of the embodiment.

[0151] That is, the distances include d4, d5 and d6 shown in FIG. **3**B, and the distance at the on-axis image height is shown as 0 mm in FIG. **8**.

[0152] As shown in FIG. **8**, in the light scanning apparatus **510** according to the aspect of the embodiment, a difference between a maximum value and a minimum value of the distances is 2.0 μm.

[0153] Then, the difference corresponds to a deviation of about 9.2% with respect to the 1200 dpi, namely a pitch of 21.2 μm, and a deviation of about 2.3% with respect to 300 dpi, namely a pitch of 84.7 μm.

[0154] Therefore, an influence of the deviation of the arrival position of each light beam on the scanned surface **1108** on the image quality can be reduced.

[0155] As described above, in the light scanning apparatus **510** according to the aspect of the embodiment, it is possible to suppress a deterioration of the image quality due to the deviation of the arrival position of each light beam on the scanned surface **1108** by satisfying Inequality (11).

Fourth Embodiment

[0156] Each of FIGS. **9**A and **9**B shows a schematic partially developed view in the main scanning cross section of a light scanning apparatus **710** according to a fourth embodiment of the disclosure.

[0157] FIGS. **10** and **11** show a schematic partial developed view in the sub-scanning cross section and a schematic partial sub-scanning cross sectional view of the light scanning apparatus **710** according to the fourth embodiment, respectively.

[0158] The light scanning apparatus **710** according to the aspect of the embodiment includes first and second light sources **101** and **201**, first and second anamorphic collimator lenses **102** and **202**, and first and second sub-scanning stops **103** and **203**.

[0159] Further, the light scanning apparatus **710** according to the aspect of the embodiment includes first and second main scanning stops **104** and **204**, a deflecting unit **1**, first fθ lenses **106** and **206**, and second fθ lenses **107** and **207**.

[0160] On optical paths, the first fθ lens **106** is arranged between the deflecting unit **1** and the second fθ lens **107**, and the first fθ lens **206** is arranged between the deflecting unit **1** and the second fθ lens **207**.

[0161] As each of the first and second light sources **101** and **201**, a semiconductor laser (multibeam laser) or the like having a plurality of light emitting points is used.

[0162] The first and second anamorphic collimator lenses **102** and **202** convert light fluxes LA and LB emitted from the first and second light sources **101** and **201** into parallel light fluxes in the main scanning cross section, respectively, and condense the light fluxes LA and LB in the sub-scanning cross section, respectively. The parallel light flux includes not only a strictly parallel light flux but also a substantially parallel light flux such as a weakly divergent light flux or a weakly convergent light flux.

[0163] The first and second sub-scanning stops **103** and **203** limit light flux diameters in the sub-scanning direction of the light fluxes LA and LB that have passed through the first and second anamorphic collimator lenses **102** and **202**, respectively.

[0164] The first and second main scanning stops **104** and **204** limit light flux diameters in the main scanning direction of the light fluxes LA and LB that have passed through the first and second sub-scanning stops **103** and **203**, respectively.

[0165] In this way, the light fluxes LA and LB emitted from the first and second light sources **101** and **201** are condensed in the sub-scanning direction in the vicinity of a first deflecting surface of the deflecting unit **1**, thereby line images elongated in the main scanning direction are formed.

[0166] The deflecting unit **1** deflects the incident light fluxes LA and LB with rotating by a driving unit such as a motor (not shown) in a direction indicated by an arrow A in FIGS. **9**A and **9**B. The deflecting unit **1** is formed by a polygon mirror, for example.

[0167] The first fθ lens **106** (first optical element, first imaging optical element) and the second fθ lens **107** are anamorphic imaging lenses having different powers between the main scanning cross section and the sub-scanning cross section, and condense (guide) the light flux LA deflected by the first deflecting surface of the deflecting unit **1** onto the first scanned surface **108**.

[0168] The first fθ lens **206** (second optical element, second imaging optical element) and the second fθ lens **207** are anamorphic imaging lenses having different powers between the main scanning cross section and the sub-scanning cross section, and condense (guide) the light flux LB deflected by the first deflecting surface of the deflecting unit **1** onto the second scanned surface **208**.

[0169] In the light scanning apparatus **710** according to the aspect of the embodiment, a first incident optical system **45***a* is formed by the first anamorphic collimator lens **102**, the first sub-scanning stop **103** and the first main scanning stop **104**.

[0170] A second incident optical system **55***a* is formed by the second anamorphic collimator lens **202**, the second sub-scanning stop **203** and the second main scanning stop **204**.

[0171] Further, in the light scanning apparatus **710** according to the aspect of the embodiment, a first scanning optical system **45***b* is formed by the first fθ lens **106** and the second fθ lens **107**.

[0172] A second scanning optical system **55***b* is formed by the first fθ lens **206** and the second fθ lens **207**.

[0173] Note that the refractive powers in the sub-scanning cross section of the second fθ lenses **107** and **207** are stronger than the refractive powers in the sub-scanning cross section of the first fθ lenses **106** and **206**, namely the strongest among the first and second scanning optical systems **45***b* and **55***b*, respectively.

[0174] The light fluxes LA emitted from the respective light emitting points of the first light source **101** pass through the first incident optical system **45***a* to be incident on the first deflecting surface of the deflecting unit **1**.

[0175] Then, the light fluxes LA incident on the first deflecting surface of the deflecting unit **1** from the first light source **101** are deflected by the first deflecting surface of the deflecting unit **1** to be guided onto the first scanned surface **108** by the first scanning optical system **45***b*, thereby the first scanned surface **108** is scanned at a constant speed.

[0176] The light fluxes LB emitted from the respective light emitting points of the second light source **201** pass through the second incident optical system **55***a* to be incident on the first deflecting surface of the deflecting unit **1**.

[0177] Then, the light fluxes LB incident on the first deflecting surface of the deflecting unit **1** from the second light source **201** are deflected by the first deflecting surface of the deflecting unit **1** to be guided onto the second scanned surface **208** by the second scanning optical system **55***b*, thereby the second scanned surface **208** is scanned at a constant speed.

[0178] Since the deflecting unit **1** rotates in the direction indicated by the arrow A in FIGS. **9**A and **9**B, the light fluxes LA and LB deflected by the deflecting unit **1** scan the first and second scanned surfaces **108** and **208** in a direction indicated by an arrow B in FIGS. **9**A and **9**B, respectively.

[0179] In FIG. **9**A and FIG. **9**B, CO represents a deflection point (on-axis deflection point) on the first deflecting surface of the deflecting unit **1** with respect to a principal ray of an on-axis light flux. The deflection point CO serves as a reference point for the first and second scanning optical systems **45***b* and **55***b*.

[0180] In the aspect of the embodiment, first and second photosensitive drums **108** and **208** are used as the first and second scanned surfaces **108** and **208**.

[0181] Exposure distributions in the sub-scanning direction on the first and second photosensitive drums **108** and **208** are formed by rotating the first and second photosensitive drums **108** and **208** in the sub-scanning direction for each main scanning exposure.

[0182] Next, various characteristics of the first and second incident optical systems **45***a* and **55***a* and the first and second scanning optical systems **45***b* and **55***b* provided in the light scanning apparatus **710** according to the aspect of the embodiment are shown in the following Tables 7 to 9.

TABLE 7

Characteristics of first and second light sources 101 and 102		
Wavelength	λ(nm)	790
Incident polarization to first deflecting surface of deflecting unit 1		p polarization
Full angle at half maximum in main scanning direction	FFPy(deg)	12.00
Full angle at half maximum in sub-scanning direction	FFPz(deg)	30.00

Shape of stop		
	Main scanning direction	Sub-scanning direction
First and second sub-scanning stops 103 and 203	10.000	2.840

TABLE 7-continued

First and second main scanning stops 104 and 204	3.750	—

Refractive index		
First and second anamorphic collimator lenses 102 and 202	N1	1.5282

Shape of optical element			
		Main scanning direction	Sub-scanning direction
Curvature radius of incident surface of first and second anamorphic collimator lenses 102 and 202	r1a (mm)	∞	∞
Curvature radius of exit surface of first and second anamorphic collimator lenses 102 and 202	r1b (mm)	−37.169	−26.170
Phase coefficient of incident surface of first and second anamorphic collimator lenses 102 and 202	D2, 0 D0, 2	−7.847E−03 —	— −8.669E−03

Focal length			
		Main scanning direction	Sub-scanning direction
First and second anamorphic collimator lenses 102 and 202	fcol (mm)	33.94	27.15

Arrangement		
First and second light sources 101 and 201 - Incident surface of first and second anamorphic collimator lenses 102 and 202	d0 (mm)	33.59
Incident surface of first and second anamorphic collimator lenses 102 and 202 - Exit surface of first and second anamorphic collimator lenses 102 and 202	d1 (mm)	3.00
Exit surface of first and second anamorphic collimator lenses 102 and 202 - First and second sub-scanning stops 103 and 203	d2 (mm)	15.15
First and second sub-scanning stops 103 and 203 - First and second main scanning stops 104 and 204	d4 (mm)	29.87
First and second main scanning stops 104 and 204 - First deflecting surface of deflecting unit 1	d5 (mm)	80.09
Incident angle in main scanning cross section of light flux LA exiting from first main scanning stop 104 to first deflecting surface	A1 (deg)	78.00
Incident angle in main scanning cross section of light flux LB exiting from second main scanning stop 204 to first deflecting surface	A2 (deg)	78.00
Incident angle in sub-scanning cross section of light flux LA exiting from first main scanning stop 104 to first deflecting surface	A3 (deg)	2.70
Incident angle in sub-scanning cross section of light flux LB exiting from second main scanning stop 204 to first deflecting surface	A4 (deg)	−2.70

TABLE 8

fθ coefficient, Scanning width, Maximum angle of view		
fθ coefficient	k (mm/rad)	207
Scanning width	W (mm)	330
Maximum angle of view	θ(deg)	45.7
Refractive index		
Refractive index of first fθ lens 106	N5	1.52819
Refractive index of second fθ lens 107	N6	1.52819
Deflecting unit 1		
Number of deflecting surfaces		4
Circumscribed radius	Rpol (mm)	10
Rotation center - Deflection reference point C0 (Optical axis direction)	Xpol (mm)	6.03
Rotation center - Deflection reference point C0 (main scanning direction)	Ypol (mm)	3.79
Arrangement in first scanning optical system 45b		
Deflection reference point C0 - Incident surface of first fθ lens 106	d12 (mm)	26.00
Incident surface of first fθ lens 106 - Exit surface of first fθ lens 106	d13 (mm)	8.20
Exit surface of first fθ lens 106 - Incident surface of second fθ lens 107	d14 (mm)	87.80
Incident surface of second fθ lens 107 - Exit surface of second fθ lens 107	d15 (mm)	4.30
Exit surface of second fθ lens 107 - First scanned surface 108	d16 (mm)	106.70
Deflection reference point C0 - Incident surface of first fθ lens 106	L1(mm)	26.00
Deflection reference point C0 - Incident surface of second fθ lens 107	L2(mm)	122.00
Deflection reference point C0 - First scanned surface 108	T2(mm)	233.00
Sub-scanning eccentricity of second fθ lens 107	shiftZ(mm)	7.21

Meridional line shape of first fθ lens 106			Meridional line shape of first fθ lens 107		
	Incident surface Opposite light source side	Exit surface Opposite light source side		Incident surface Opposite light source side	Exit surface Opposite light source side
R	−71.101	−43.800	R	−4000	379.967
ku	9.464E−01	−9.321E−01	ku	0	−7.412E+01
B4u	−9.147E−07	1.355E−06	B4u	0	−1.332E−07
B6u	6.784E−09	1.719E−09	B6u	0	7.206E−12
B8u	−5.767E−12	8.761E−13	B8u	0	−3.070E−16
B10u	1.638E−15	−1.069E−15	B10u	0	6.089E−21
B12u	0	0	B12u	0	0.000E+00
	Light source side	Light source side		Light source side	Light source side
k1	9.464E−01	−9.321E−01	k1	0	−7.412E+01
B41	−9.147E−07	−1.355E−06	B41	0	−1.332E−07
B61	6.784E−09	1.719E−09	B61	0	7.206E−12

TABLE 8-continued

B81	−5.767E−12	8.761E−13	B81	0	−3.070E−16
B101	1.638E−15	−1.069E−15	B101	0	6.089E−21
B121	0	0	B121	0	0.000E+00

Sagittal line shape of first fθ lens 106			Sagittal line shape of second fθ lens 107		
	Incident surface Sagittal line R change	Exit surface Sagittal line R change		Incident surface Sagittal line R change	Exit surface Sagittal line R change
r	20.000	55.261	r	37.426	−249.9931
E1	0	0	E1	0.000E+00	9.40981E−09
E2	0	6.894E−06	E2	−3.482E−07	1.44641E−06
E3	0	0	E3	0	−1.61579E−09
E4	0	8.425E−08	E4	0.000E+00	−2.7926E−10
E5	0	0	E5	0	4.72069E−13
E6	0	−2.679E−10	E6	0.000E+00	4.45476E−14
E7	0	0	E7	0	−5.35403E−17
E8	0	3.4364E−13	E8	0.000E+00	−3.93574E−18
E9	0	0	E9	0	2.02748E−21
E10	0	−1.53852E−16	E10	0	1.36304E−22
	Sagittal line tilt	Sagittal line tilt		Sagittal line tilt	Sagittal line tilt
M0_1	0	7.661E−02	M0_1	1.211E−01	−5.801E−02
M1_1	0	0.000E+00	M1_1	2.129E−04	2.002E−04
M2_1	0	−3.906E−05	M2_1	1.111E−05	2.292E−05
M3_1	0	0.000E+00	M3_1	−1.419E−07	−1.288E−07
M4_1	0	0.000E+00	M4_1	−5.557E−10	−2.627E−09
M5_1	0	0	M5_1	2.589E−11	2.174E−11
M6_1	0	0	M6_1	−2.459E−13	2.067E−13
M7_1	0	0	M7_1	−2.150E−15	−1.675E−15
M8_1	0	0	M8_1	1.182E−17	−3.209E−17
M9_1	0	0	M9_1	6.130E−20	4.199E−20
M10_1	0	0	M10_1	9.717E−23	1.487E−21
M11_1	0	0	M11_1	0	0
M12_1	0	0	M12_1	0	0

TABLE 9

fθ coefficient, Scanning width, Maximum angle of view		
fθ coefficient	k (mm/rad)	207
Scanning width	W (mm)	330
Maximum angle of view	θ(deg)	45.7
Refractive index		
Refractive index of first fθ lens 206	N5	1.52819
Refractive index of second fθ lens 207	N6	1.52819
Deflecting unit 1		
Number of deflecting surfaces		4
Circumscribed radius	Rpol (mm)	10
Rotation center - Deflection reference point C0 (Optical axis direction)	Xpol (mm)	6.03
Rotation center - Deflection reference point C0 (main scanning direction)	Ypol (mm)	3.79
Arrangement in second scanning optical system 55b		
Deflection reference point C0 - Incident surface of first fθ lens 206	d12 (mm)	26.00
Incident surface of first fθ lens 206 - Exit surface of first fθ lens 206	d13 (mm)	8.20

TABLE 9-continued

Exit surface of first fθ lens 206 - Incident surface of second fθ lens 207	d14 (mm)	69.30
Incident surface of second fθ lens 207 - Exit surface of second fθ lens 207	d15 (mm)	4.30
Exit surface of second fθ lens 207 - Second scanned surface 208	d16 (mm)	125.20
Deflection reference point C0 - Incident surface of first fθ lens 206	L3(mm)	26.00
Deflection reference point C0 - Incident surface of second fθ lens 207	L4(mm)	103.50
Deflection reference point C0 - Second scanned surface 208	T2(mm)	233.00
Sub-scanning eccentricity of second fθ lens 207	shiftZ(mm)	5.03

	Meridional line shape of second fθ lens 206			Meridional line shape of second fθ lens 207	
	Incident surface Opposite light source side	Exit surface Opposite light source side		Incident surface Opposite light source side	Exit surface Opposite light source side
R	−71.101	−42.946	R	−4000	350.123
ku	9.464E−01	−5.155E−01	ku	0	−8.753E+01
B4u	−9.147E−07	−3.477E−07	B4u	0	−2.020E−07
B6u	6.784E−09	1.690E−09	B6u	0	1.609E−11
B8u	−5.767E−12	1.110E−12	B8u	0	−9.313E−16
B10u	1.638E−15	−1.224E−15	B10u	0	2.524E−20
B12u	0	0	B12u	0	0
	Light source side	Light source side		Light source side	Light source side
k1	9.464E−01	−5.155E−01	k1	0	−8.753E+01
B41	−9.147E−07	−3.477E−07	B41	0	−2.020E−07
B61	6.784E−09	1.690E−09	B61	0	1.609E−11
B81	−5.767E−12	1.110E−12	B81	0	−9.313E−16
B101	1.638E−15	−1.224E−15	B101	0	2.524E−20
B121	0	0	B121	0	0

	Sagittal line shape of first fθ lens 206			Sagittal line shape of second fθ lens 207	
	Incident surface Sagittal line R change	Exit surface Sagittal line R change		Incident surface Sagittal line R change	Exit surface Sagittal line R change
r	20.000	25.004	r	37.079	−154.0078
E1	0	0	E1	0	−1.27778E−07
E2	0	1.522E−05	E2	−7.458E−07	1.81313E−06
E3	0	0	E3	0	−3.2397E−09
E4	0	8.486E−10	E4	0	−3.04103E−10
E5	0	0	E5	0	1.33875E−12
E6	0	−2.508E−11	E6	0	3.08183E−14
E7	0	0	E7	0	−2.00884E−16
E8	0	7.60678E−15	E8	0	−1.95419E−18
E9	0	0	E9	0	9.85865E−21
E10	0	1.60971E−17	E10	0	5.81192E−23
	Sagittal line tilt	Sagittal line tilt		Sagittal line tilt	Sagittal line tilt
M0_1	0	2.124E−02	M0_1	−1.007E−01	2.315E−02
M1_1	0	0	M1_1	−2.129E−04	−2.002E−04
M2_1	0	−3.321E−05	M2_1	−1.314E−05	−2.370E−05
M3_1	0	0	M3_1	1.161E−07	1.056E−07
M4_1	0	0	M4_1	1.765E−09	3.675E−09
M5_1	0	0	M5_1	−1.616E−11	−1.409E−11

TABLE 9-continued

M6_1	0	0	M6_1	3.014E−13	−3.052E−13
M7_1	0	0	M7_1	1.061E−15	9.733E−16
M8_1	0	0	M8_1	−1.306E−17	6.574E−17
M9_1	0	0	M9_1	−1.657E−20	−1.728E−20
M10_1	0	0	M10_1	−8.536E−22	−3.960E−21
M11_1	0	0	M11_1	0	0
M12_1	0	0	M12_1	0	0

[0183] In Tables 7 to 9, an optical axis, an axis orthogonal to the optical axis in the main scanning cross section, and an axis orthogonal to the optical axis in the sub-scanning cross section are defined as an X-axis, a Y-axis, and a Z-axis, respectively, when an intersection between each lens surface and the optical axis is defined as an origin.

[0184] Further, in Tables 8 and 9, "E-x" means "$\times 10^{-x}$".

[0185] An aspheric surface shape (meridional line shape) in the main scanning cross section of each lens surface of the first fθ lenses **106** and **206** and the second fθ lenses **107** and **207** provided in the light scanning apparatus **710** according to the aspect of the embodiment is expressed by the above-described Expression (1).

[0186] An aspheric surface shape (sagittal line shape) in the sub-scanning cross section of each lens surface of the first fθ lenses **106** and **206** and the second fθ lenses **107** and **207** provided in the light scanning apparatus **710** according to the aspect of the embodiment is expressed by the above-described Expression (2).

[0187] A curvature radius r' in the sub-scanning cross section of each lens surface of the first fθ lenses **106** and **206** and the second fθ lenses **107** and **207** provided in the light scanning apparatus **710** according to the aspect of the embodiment continuously varies in accordance with a position in the Y direction as expressed by the above-described Expression (3).

[0188] Each of the first and second anamorphic collimator lenses **102** and **202** provided in the light scanning apparatus **710** according to the aspect of the embodiment has an incident surface formed by a diffracting surface defined by an optical path difference function of two variables Y and Z as expressed by the above-described Expression (4).

[0189] Further, Inequality (11) be satisfied in the first incident optical system **45***a* and the first scanning optical system **45***b* provided in the light scanning apparatus **710** according to the aspect of the embodiment.

[0190] In other words, an inclination at the arrival position of the light beam from the i-th light emitting point of the first light source **101** on the exit surface (first sagittal line tilt surface, first optical surface) of the first fθ lens **106** provided in the light scanning apparatus **710** according to the aspect of the embodiment is represented by M_{1i}. A lateral magnification in the sub-scanning cross section of the first incident optical system **45***a* is represented by β_1.

[0191] A distance on the optical axis of the first incident optical system **45***a* between the first light source **101** and the first deflecting surface of the deflecting unit **1** provided in the light scanning apparatus **710** according to the aspect of the embodiment is represented by L_1 (mm).

[0192] A distance on the optical axis of the first scanning optical system **45***b* between the first deflecting surface of the deflecting unit **1** and the exit surface of the first fθ lens **106** provided in the light scanning apparatus **710** according to the aspect of the embodiment is represented by D_1 (mm).

[0193] At this time, in the first incident optical system **45***a* and the first scanning optical system **45***b* provided in the light scanning apparatus **710** according to the aspect of the embodiment, the following Inequality (11c) be satisfied:

$$0.05 < \left| M_{1i}\left[-\beta_1 + \frac{(1-\beta_1)D_1}{L_1}\right]\right| < 0.70. \tag{11c}$$

[0194] In the first incident optical system **45***a* and the first scanning optical system **45***b* provided in the light scanning apparatus **710** according to the aspect of the embodiment, Inequality (11a) be satisfied, and it is more preferred that Inequality (11b) be satisfied.

[0195] Further, in the first incident optical system **45***a* and the first scanning optical system **45***b* provided in the light scanning apparatus **710** according to the aspect of the embodiment, Inequalities (12) and (13) be satisfied.

[0196] In other words, the following Inequality (12a) be satisfied by using the aspheric surface coefficient M_{01} of the exit surface of the first fθ lens **106** provided in the light scanning apparatus **710** according to the aspect of the embodiment:

$$0 < \left| M_{01}\left[-\beta_1 + \frac{(1-\beta_1)D_1}{L_1}\right]\right| < 0.185. \tag{12a}$$

[0197] Further, in other words, a curvature radius in the sub-scanning cross section of the exit surface of the first fθ lens **106** on the optical axis of the first scanning optical system **45***b* is represented by R (mm), and an eccentricity amount in the sub-scanning direction of the first fθ lens **106** is represented by L_s (mm).

[0198] At this time, the following Inequality (13a) be satisfied:

$$0.05 < \left| \left[\frac{L_s}{R} + M_{01}\right] \times \left[-\beta_1 + \frac{(1-\beta_1)D_1}{L_1}\right]\right| < 0.70. \tag{13a}$$

[0199] Specifically, in the first incident optical system **45***a* and the first scanning optical system **45***b* provided in the light scanning apparatus **710** according to the aspect of the embodiment, β is −3.65, D is 34.2 mm, Lis 161.7 mm, and M is 0.100.

[0200] Therefore, the value of each of Inequalities (11), (11a) and (11b) is calculated as 0.465, so that Inequalities (11), (11a) and (11b) are satisfied.

[0201] On the other hand, in the first incident optical system **45***a* and the first scanning optical system **45***b* provided in the light scanning apparatus **710** according to the aspect of the embodiment, since M_{01} is 0.0766, the value of Inequality (12) is calculated as 0.355, so that Inequality (12) is not satisfied.

[0202] Further, in the first incident optical system **45***a* and the first scanning optical system **45***b* provided in the light scanning apparatus **710** according to the aspect of the embodiment, L_s is 1.31 mm and R is 55.261 mm. Therefore, the value of Inequality (13) is calculated as 0.465, so that Inequality (13) is satisfied.

[0203] In addition, in the second incident optical system **55***a* and the second scanning optical system **55***b* provided in the light scanning apparatus **710** according to the aspect of the embodiment, Inequality (11) be satisfied.

[0204] In other words, an inclination at the arrival position of the light beam from the j-th light emitting point of the second light source **201** on the exit surface (second sagittal line tilt surface, second optical surface) of the first fθ lens **206** provided in the light scanning apparatus **710** according to the aspect of the embodiment is represented by M_{2j}.

[0205] A lateral magnification in the sub-scanning cross section of the second incident optical system **55***a* is represented by β_2.

[0206] A distance on the optical axis of the second incident optical system **55***a* between the second light source **201** and the first deflecting surface of the deflecting unit **1** provided in the light scanning apparatus **710** according to the aspect of the embodiment is represented by L_2 (mm).

[0207] A distance on the optical axis of the second scanning optical system **55***b* between the first deflecting surface of the deflecting unit **1** and the exit surface of the first fθ lens **206** provided in the light scanning apparatus **710** according to the aspect of the embodiment is represented by D_2 (mm).

[0208] At this time, in the second incident optical system **55***a* and the second scanning optical system **55***b* provided in the light scanning apparatus **710** according to the aspect of the embodiment, the following Inequality (11d) be satisfied:

$$0.05 < \left| M_{2j}\left[-\beta_2 + \frac{(1-\beta_2)D_2}{L_2} \right] \right| < 0.70. \tag{11d}$$

[0209] Further, in the second incident optical system **55***a* and the second scanning optical system **55***b* provided in the light scanning apparatus **710** according to the aspect of the embodiment, Inequality (11a) be satisfied, and it is more preferred that Inequality (11b) be satisfied.

[0210] In addition, in the second incident optical system **55***a* and the second scanning optical system **55***b* provided in the light scanning apparatus **710** according to the aspect of the embodiment, Inequalities (12) and (13) be satisfied.

[0211] Specifically, in the second incident optical system **55***a* and the second scanning optical system **55***b* provided in the light scanning apparatus **710** according to the aspect of the embodiment, β is −3.65, D is 34.2 mm, Lis 161.7 mm, and M is 0.0735.

[0212] Therefore, the value of each of Inequalities (11), (11a) and (11b) is calculated as 0.341, so that Inequalities (11), (11a) and (11b) are satisfied.

[0213] Further, in the second incident optical system **55***a* and the second scanning optical system **55***b* provided in the light scanning apparatus **710** according to the aspect of the embodiment, since M_{01} is 0.0212, the value of Inequality (12) is calculated as 0.098, so that Inequality (12) is satisfied.

[0214] Furthermore, in the second incident optical system **55***a* and the second scanning optical system **55***b* provided in the light scanning apparatus **710** according to the aspect of the embodiment, since L_s is 1.31 mm and R is 25.004 mm, the value of Inequality (13) is calculated as 0.341, so that Inequality (13) is satisfied.

[0215] Note that, in the light scanning apparatus **710** according to the aspect of the embodiment, an absolute value of the sagittal line tilt amount M_{01} on the optical axis of the exit surface of the first fθ lens **106** and an absolute value of the sagittal line tilt amount M_{01} on the optical axis of the exit surface of the first fθ lens **206** are different from each other.

[0216] FIG. **12**A shows distances in the main scanning direction between the arrival position of the light beam **2105***a* and the arrival position of the light beam **2105***b* at the respective image heights on the first scanned surface **108** in the light scanning apparatus **710** according to the aspect of the embodiment.

[0217] That is, the distances include d4, d5, and do shown in FIG. **3**B, and the distance at the on-axis image height is shown as 0 mm in FIG. **12**A.

[0218] FIG. **12**B shows distances in the main scanning direction between the arrival position of the light beam **2105***a* and the arrival position of the light beam **2105***b* at the respective image heights on the second scanned surface **208** in the light scanning apparatus **710** according to the aspect of the embodiment.

[0219] That is, the distances include d4, d5, and d6 shown in FIG. **3**B, and the distance at the on-axis image height is shown as 0 mm in FIG. **12**B.

[0220] As shown in FIG. **12**A, in the light scanning apparatus **710** according to the aspect of the embodiment, a difference between a maximum value and a minimum value of the distances on the first scanned surface **108** is 6.3 μm.

[0221] Since the difference corresponds to a deviation of about 7.4% with respect to 300 dpi, namely a pitch of 84.7 μm, an influence of the deviation of the arrival position of each light beam on the first scanned surface **108** on the image quality can be reduced.

[0222] Further, as shown in FIG. **12**B, in the light scanning apparatus **710** according to the aspect of the embodiment, a difference between a maximum value and a minimum value of the distances on the second scanned surface **208** is 2.0 μm.

[0223] Since the difference corresponds to a deviation of about 2.3% with respect to 300 dpi, namely the pitch of 84.7 μm, an influence of the deviation of the arrival position of each light beam on the second scanned surface **208** on the image quality can be reduced.

[0224] As described above, in the light scanning apparatus **710** according to the aspect of the embodiment, Inequalities (11) and (13) are satisfied for the first incident optical system **45***a* and the first scanning optical system **45***b*.

[0225] On the other hand, all of Inequalities (11), (12) and (13) are satisfied for the second incident optical system **55***a* and the second scanning optical system **55***b*.

[0226] This makes it possible to reduce the distances in the main scanning direction between the arrival position of the light beam **2105***a* and the arrival position of the light beam **2105***b* at the respective image heights on the second scanned surface **208** than on the first scanned surface **108**.

[0227] As described above, in the light scanning apparatus **710** according to the aspect of the embodiment, Inequality (11) is satisfied in the first incident optical system **45***a* and the first scanning optical system **45***b*, thereby it is possible to suppress a deterioration of the image quality due to the deviation of the arrival position of each light beam on the first scanned surface **108**.

[0228] Further, in the light scanning apparatus **710** according to the aspect of the embodiment, Inequality (11) is satisfied in the second incident optical system **55***a* and the second scanning optical system **55***b*, thereby it is possible to suppress a deterioration of the image quality due to the deviation of the arrival position of each light beam on the second scanned surface **208**.

Fifth Embodiment

[0229] FIG. **13** shows a schematic developed view in the main scanning cross section of a light scanning apparatus **910** according to a fifth embodiment of the disclosure.

[0230] FIGS. **14** and **15** show a schematic partial developed view in the sub-scanning cross section and a schematic partial sub-scanning cross sectional view of the light scanning apparatus **910** according to the fifth embodiment, respectively.

[0231] The light scanning apparatus **910** according to the aspect of the embodiment includes first, second, third and fourth light sources **301**, **401**, **501** and **601**, and first, second, third and fourth anamorphic collimator lenses **302**, **402**, **502** and **602**.

[0232] Further, the light scanning apparatus **910** according to the aspect of the embodiment includes first, second, third and fourth sub-scanning stops **303**, **403**, **503**, and **603**, and first, second, third and fourth main scanning stops **304**, **404**, **504** and **604**.

[0233] Furthermore, the light scanning apparatus **910** according to the aspect of the embodiment includes a deflecting unit **1**, first fθ lenses **306**, **406**, **506** and **606**, second fθ lenses **307**, **407**, **507** and **607**, and folding mirrors **311**, **312**, **411**, **511**, **512** and **611**.

[0234] On optical paths, the first fθ lens **306** is arranged between the deflecting unit **1** and the second fθ lens **307**, and the first fθ lens **406** is arranged between the deflecting unit **1** and the second fθ lens **407**.

[0235] On optical paths, the first fθ lens **506** is arranged between the deflecting unit **1** and the second fθ lens **507**, and the first fθ lens **606** is arranged between the deflecting unit **1** and the second fθ lens **607**.

[0236] As each of the first, second, third and fourth light sources **301**, **401**, **501** and **601**, a semiconductor laser or the like having a plurality of light emitting points is used.

[0237] The first, second, third and fourth anamorphic collimator lenses **302**, **402**, **502** and **602** convert the light fluxes LC, LD, LE and LF emitted from the first, second, third and fourth light sources **301**, **401**, **501** and **601** into parallel light fluxes in the main scanning cross section, respectively, and condense the light fluxes LC, LD, LE and LF in the sub-scanning cross section, respectively.

[0238] The parallel light flux includes not only a strictly parallel light flux but also a substantially parallel light flux such as a weakly divergent light flux or a weakly convergent light flux.

[0239] The first, second, third and fourth sub-scanning stops **303**, **403**, **503** and **603** limit light flux diameters in the sub-scanning direction of the light fluxes LC, LD, LE and LF that have passed through the first, second, third and fourth anamorphic collimator lenses **302**, **402**, **502** and **602**, respectively.

[0240] The first, second, third and fourth main scanning stops **304**, **404**, **504** and **604** limit light flux diameters in the main scanning direction of the light fluxes LC, LD, LE, and LF that have passed through the first, second, third and fourth sub-scanning stops **303**, **403**, **503** and **603**, respectively.

[0241] In this way, the light fluxes LC and LD emitted from the first and second light sources **301** and **401** are condensed in the sub-scanning direction in the vicinity of a first deflecting surface of the deflecting unit **1**, respectively, so that line images elongated in the main scanning direction are formed.

[0242] Further, the light fluxes LE and LF emitted from the third and fourth light sources **501** and **601** are condensed in the sub-scanning direction in the vicinity of a second deflecting surface of the deflecting unit **1**, respectively, so that line images elongated in the main scanning direction are formed.

[0243] The deflecting unit **1** deflects the incident light fluxes LC, LD, LE and LF with rotating in a direction indicated by an arrow A in FIG. **13** by a driving unit such as a motor (not shown). The deflecting unit **1** is formed by a polygon mirror, for example.

[0244] The first fθ lens **306** (first optical element, first imaging optical element) and the second fθ lens **307** are anamorphic imaging lenses having different powers between the main scanning cross section and the sub-scanning cross section, and condense (guide) the light flux LC deflected by the first deflecting surface of the deflecting unit **1** onto the first scanned surface **308**.

[0245] The first fθ lens **406** (second optical element, second imaging optical element) and the second fθ lens **407** are anamorphic imaging lenses having different powers between the main scanning cross section and the sub-scanning cross section, and condense (guide) the light flux LD deflected by the first deflecting surface of the deflecting unit **1** onto the second scanned surface **408**.

[0246] The first fθ lens **506** (third optical element, third imaging optical element) and the second fθ lens **507** are anamorphic imaging lenses having different powers between the main scanning cross section and the sub-scanning cross section, and condense (guide) the light flux LE deflected by the second deflecting surface of the deflecting unit **1** onto the third scanned surface **508**.

[0247] The first fθ lens **606** (fourth optical element, fourth imaging optical element) and the second fθ lens **607** are anamorphic imaging lenses having different powers between the main scanning cross section and the sub-scanning cross section, and condense (guide) the light flux LF deflected by the second deflecting surface of the deflecting unit **1** on the fourth scanned surface **608**.

[0248] The folding mirrors **311** and **312** reflect the light flux LC deflected by the first deflecting surface of the deflecting unit **1** so as to fold the optical path of the light flux LC, and the folding mirror **411** reflects the light flux LD deflected by the first deflecting surface of the deflecting unit **1** so as to fold the optical path of the light flux LD.

[0249] The folding mirrors **511** and **512** reflect the light flux LE deflected by the second deflecting surface of the deflecting unit **1** so as to fold the optical path of the light flux LE, and the folding mirror **611** reflects the light flux LF deflected by the second deflecting surface of the deflecting unit **1** so as to fold the optical path of the light flux LF.

[0250] In the light scanning apparatus **910** according to the aspect of the embodiment, a first incident optical system **65***a* is formed by the first anamorphic collimator lens **302**, the first sub-scanning stop **303** and the first main scanning stop **304**.

[0251] A second incident optical system **75***a* is formed by the second anamorphic collimator lens **402**, the second sub-scanning stop **403** and the second main scanning stop **404**.

[0252] A third incident optical system **85***a* is formed by the third anamorphic collimator lens **502**, the third sub-scanning stop **503** and the third main scanning stop **504**.

[0253] A fourth incident optical system **95***a* is formed by the fourth anamorphic collimator lens **602**, the fourth sub-scanning stop **603** and the fourth main scanning stop **604**.

[0254] Further, in the light scanning apparatus **910** according to the aspect of the embodiment, a first scanning optical system **65***b* is formed by the first fθ lens **306** and the second fθ lens **307**, and a second scanning optical system **75***b* is formed by the first fθ lens **406** and the second fθ lens **407**.

[0255] A third scanning optical system **85***b* is formed by the first fθ lens **506** and the second fθ lens **507**, and a fourth scanning optical system **95***b* is formed by the first fθ lens **606** and the second fθ lens **607**.

[0256] A refractive power in the sub-scanning cross section of the second fθ lenses **307**, **407**, **507** and **607** is stronger than a refractive power in the sub-scanning cross section of the first fθ lenses **306**, **406**, **506** and **606**, namely the strongest in the first, second, third and fourth scanning optical systems **65***b*, **75***b*, **85***b* and **95***b*, respectively.

[0257] The light fluxes LC emitted from the respective light emitting points of the first light source **301** pass through the first incident optical system **65***a* to be incident on the first deflecting surface of the deflecting unit **1**.

[0258] Then, the light fluxes LC incident on the first deflecting surface of the deflecting unit **1** from the first light source **301** are deflected by the first deflecting surface of the deflecting unit **1** to be guided onto the first scanned surface **308** by the first scanning optical system **65***b*, thereby the first scanned surface **308** is scanned at a constant speed.

[0259] The light fluxes LD emitted from the respective light emitting points of the second light source **401** pass through the second incident optical system **75***a* to be incident on the first deflecting surface of the deflecting unit **1**.

[0260] Then, the light fluxes LD incident on the first deflecting surface of the deflecting unit **1** from the second light source **401** are deflected by the first deflecting surface of the deflecting unit **1** to be guided onto the second scanned surface **408** by the second scanning optical system **75***b*, thereby the second scanned surface **408** is scanned at a constant speed.

[0261] The light fluxes LE emitted from the respective light emitting points of the third light source **501** pass through the third incident optical system **85***a* to be incident on the second deflecting surface of the deflecting unit **1**.

[0262] Then, the light fluxes LE incident on the second deflecting surface of the deflecting unit **1** from the third light source **501** are deflected by the second deflecting surface of the deflecting unit **1** to be guided onto the third scanned surface **508** by the third scanning optical system **85***b*, thereby the third scanned surface **508** is scanned at a constant speed.

[0263] The light fluxes LF emitted from the respective light emitting points of the fourth light source **601** pass through the fourth incident optical system **95***a* to be incident on the second deflecting surface of the deflecting unit **1**.

[0264] Then, the light fluxes LF incident on the second deflecting surface of the deflecting unit **1** from the fourth light source **601** are deflected by the second deflecting surface of the deflecting unit **1** to be guided onto the fourth scanned surface **608** by the fourth scanning optical system **95***b*, thereby the fourth scanned surface **608** is scanned at a constant speed.

[0265] Since the deflecting unit **1** rotates in the direction indicated by the arrow A in FIG. **13**, the light fluxes LC, LD, LE and LF deflected by the deflecting unit **1** scan the first, second, third and fourth scanned surfaces **308**, **408**, **508** and **608** in a direction indicated by an arrow B in FIG. **13**, respectively.

[0266] In FIGS. **13** to **15**, D0 and E0 represent deflection points (on-axis deflection points) on the first and second deflecting surfaces of the deflecting unit **1** with respect to a principal ray of an on-axis light flux, respectively.

[0267] The deflection point D0 serves as a reference point of the first and second scanning optical systems **65***b* and **75***b*, and the deflection point E0 serves as a reference point of the third and fourth scanning optical systems **85***b* and **95***b*.

[0268] In the aspect of the embodiment, first, second, third and fourth photosensitive drums **308**, **408**, **508** and **608** are used as the first, second, third and fourth scanned surfaces **308**, **408**, **508** and **608**.

[0269] Exposure distributions in the sub-scanning direction on the first, second, third and fourth photosensitive drums **308**, **408**, **508**, and **608** are formed by rotating the first, second, third and fourth photosensitive drums **308**, **408**, **508** and **608** in the sub-scanning direction for each main scanning exposure, respectively.

[0270] Next, various characteristics of the first, second, the third and fourth incident optical systems **65***a*, **75***a*, **85***a* and **95***a*, and first, second, third and fourth scanning optical systems **65***b*, **75***b*, **85***b* and **95***b* provided in the light scanning apparatus **910** according to the aspect of the embodiment are shown in the following Tables 10 to 12.

TABLE 10

Characteristics of first, second, third and fourth light sources 301, 401, 501 and 601		
Wavelength	λ(nm)	790
Incident polarization to first and second deflecting surfaces of deflecting unit 1		p polarization
Full angle at half maximum in main scanning direction	FFPy(deg)	12.00
Full angle at half maximum in sub-scanning direction	FFPz(deg)	30.00
Shape of stop		
	Main scanning direction	Sub-scanning direction
First, second, third and fourth sub-scanning stops 303, 403, 503 and 603	10.000	2.840

TABLE 10-continued

First, second, third and fourth main scanning stops 304, 404, 504 and 604		3.750	—
Refractive index			
First, second, third and fourth anamorphic collimator lenses 302, 402, 502 and 602	N1	1.5282	
Shape of optical element			
		Main scanning direction	Sub-scanning direction
Curvature radius of incident surface of first, second, third and fourth anamorphic collimator lenses 302, 402, 502 and 602	r1a (mm)	∞	∞
Curvature radius of exit surface of first, second, third and fourth anamorphic collimator lenses 302, 402, 502 and 602	r1b (mm)	−37.169	−26.170
Phase coefficient of incident surface of first, second, third and fourth anamorphic collimator lenses 302, 402, 502 and 602	D2, 0	−7.847E−03	—
	D0, 2	—	−8.669E−03
Focal length			
		Main scanning direction	Sub-scanning direction
First to fourth anamorphic collimator lenses 302 to 602	fcol (mm)	33.94	27.15
Arrangement			
First to fourth light sources 301 to 601 - Incident surface of first to fourth anamorphic collimator lenses 302 to 602	d0 (mm)	33.59	
Incident surface of first to fourth anamorphic collimator lenses 302 to 602 - Exit surface of first to fourth anamorphic collimator lenses 302 to 602	d1 (mm)	3.00	
Exit surface of first to fourth anamorphic collimator lenses 302 to 602 - First to fourth sub-scanning stops 303 to 603	d2 (mm)	15.15	
First to fourth sub-scanning stops 303 to 603 - First to fourth main scanning stop 304 to 604	d4 (mm)	29.87	
First to fourth main scanning stop 304 to 604 - First and second deflecting surfaces of deflecting unit 1	d5 (mm)	80.09	
Incident angle in main scanning cross section of light flux LC exiting from first main scanning stop 304 to first deflecting surface	A1 (deg)	78.00	
Incident angle in main scanning cross section of light flux LD exiting from second main scanning stop 404 to first deflecting surface	A2 (deg)	78.00	
Incident angle in main scanning cross section of light flux LE exiting from third main scanning stop 504 to second deflecting surface	A3 (deg)	102.00	
Incident angle in main scanning cross section of light flux LF exiting from fourth main scanning stop 604 to second deflecting surface	A4 (deg)	102.00	
Incident angle in sub-scanning cross section of light flux LC exiting from first main scanning stop 304 to first deflecting surface	A5 (deg)	2.70	
Incident angle in sub-scanning cross section of light flux LD exiting from second main scanning stop 404 to first deflecting surface	A6 (deg)	−2.70	
Incident angle in sub-scanning cross section of light flux LE exiting from third main scanning stop 504 to second deflecting surface	A7 (deg)	−2.70	
Incident angle in sub-scanning cross section of light flux LF exiting from fourth main scanning stop 604 to second deflecting surface	A8 (deg)	2.70	

TABLE 11

fθ coefficient, Scanning width, Maximum angle of view		
fθ coefficient	k (mm/rad)	207
Scanning width	W (mm)	330
Maximum angle of view	θ(deg)	45.7
Refractive index		
Refractive index of first fθ lenses 306 and 506	N5	1.52819
Refractive index of second fθ lenses 307 and 507	N6	1.52819
Deflecting unit 1		
Number of deflecting surfaces		4
Circumscribed radius	Rpol (mm)	10
Rotation center - Deflection reference points D0 and E0 (Optical axis direction)	Xpol (mm)	6.03
Rotation center - Deflection reference points D0 and E0 (main scanning direction)	Ypol (mm)	3.79
Arrangement in first and third scanning optical systems 65b and 85b		
Deflection reference points D0 and E0 - Incident surface of first fθ lenses 306 and 506	d12 (mm)	26.00
Incident surface of first fθ lenses 306 and 506 - Exit surface of first fθ lenses 306 and 506	d13 (mm)	8.20
Exit surface of first fθ lenses 306 and 506 - Incident surface of second fθ lenses 307 and 507	d14 (mm)	87.80

TABLE 11-continued

Incident surface of second fθ lenses 307 and 507 - Exit surface of second fθ lenses 307 and 507	d15 (mm)	4.30
Exit surface of second fθ lenses 307 and 507 - First and third scanned surfaces 308 and 508	d16 (mm)	106.70
Deflection reference points D0 and E0 - Incident surface of first fθ lenses 306 and 506	L1 (mm)	26.00
Deflection reference points D0 and E0 - Incident surface of second ff lenses 307 and 507	L2 (mm)	122.00
Deflection reference points D0 and E0 - First and third scanned surfaces 308 and 508	T2 (mm)	233.00
Sub-scanning eccentricity of second fθ lenses 307 and 507	shiftZ (mm)	9.06

	Meridional line shape of first fθ lenses 306 and 506			Meridional line shape of second fθ lenses 307 and 507	
	Incident surface Opposite light source side	Exit surface Opposite light source side		Incident surface Opposite light source side	Exit surface Opposite light source side
R	−71.974	−44.323	R	−4000	383.925
Ku	8.921E−01	−1.162E+00	ku	0	−7.626E+01
B4u	−7.612E−07	−1.519E−06	B4U	0	−1.344E−07
B6u	6.789E−09	1.750E−09	B6u	0	7.455E−12
B8u	−5.889E−12	9.640E−13	B8u	0	−3.304E−16
B10u	1.617E−15	−1.195E−15	B10u	0	7.016E−21
B12u	0	0	B12u	0	0.000E+00
	Light source side	Light source side		Light source side	Light source side
k1	8.921E−01	−1.162E+00	k1	0	−7.626E+01
B41	−7.612E−07	−1.519E−06	B41	0	−1.344E−07
B61	6.789E−09	1.750E−09	B61	0	7.455E−12
B81	−5.889E−12	9.640E−13	B81	0	−3.304E−16
B101	1.617E−15	−1.195E−15	B101	0	7.016E−21
B121	0	0	B121	0	0.000E+00

	Sagittal line shape of first fθ lenses 306 and 506			Sagittal line shape of first fθ lenses 307 and 507	
	Incident surface Sagittal line R change	Exit surface Sagittal line R change		Incident surface Sagittal line R change	Exit surface Sagittal line R change
r	20.000	54.586	r	46.180	−110.3864
E1	0	0	E1	0	−7.53378E−07
E2	0	3.970E−06	E2	5.267E−09	1.78758E−06
E3	0	0	E3	0	−7.47644E−10
E4	0	9.864E−08	E4	0	−2.81187E−10
E5	0	0	E5	0	1.8249E−13
E6	0	−2.887E−10	E6	0	4.07154E−14
E7	0	0	E7	0	−1.73958E−17
E8	0	3.62156E−13	E8	0	−3.24923E−18
E9	0	0	E9	0	5.08768E−22
E10	0	−1.61888E−16	E10	0	9.97713E−23
	Sagittal line tilt	Sagittal line tilt		Sagittal line tilt	Sagittal line tilt
M0_1	0	1.136E−01	M0_1	1.499E−01	−7.953E−02
M1_1	0	0	M1_1	2.041E−05	1.318E−05
M2_1	0	−5.071E−05	M2_1	3.507E−08	1.547E−05
M3_1	0	0	M3_1	−4.837E−08	−4.462E−08
M4_1	0	0	M4_1	5.229E−10	−1.812E−09
M5_1	0	0	M5_1	1.018E−11	8.807E−12
M6_1	0	0	M6_1	−2.073E−13	1.663E−13
M7_1	0	0	M7_1	−9.447E−16	−7.761E−16
M8_1	0	0	M8_1	2.868E−18	−2.426E−17
M9_1	0	0	M9_1	2.861E−20	2.113E−20
M10_1	0	0	M10_1	−7.599E−23	4.798E−22
M11_1	0	0	M11_1	0	0
M12_1	0	0	M12_1	0	0

TABLE 12

fθ coefficient, Scanning width, Maximum angle of view		
fθ coefficient	k (mm/rad)	207
Scanning width	W (mm)	330
Maximum angle of view	θ(deg)	45.7

Refractive index		
Refractive index of first fθ lenses 406 and 406	N5	1.52819
Refractive index of second fθ lenses 407 and 607	N6	1.52819

Deflecting unit 1		
Number of deflecting surfaces		4
Circumscribed radius	Rpol (mm)	10
Rotation center - Deflection reference points D0 and E0 (Optical axis direction)	Xpol (mm)	−6.03
Rotation center - Deflection reference points D0 and E0 (main scanning direction)	Ypol (mm)	3.79

Arrangement in second and fourth scanning optical systems 75b and 95b		
Deflection reference points D0 and E0 - Incident surface of first fθ lenses 406 and 606	d12 (mm)	26.00
Incident surface of first fθ lenses 406 and 606 - Exit surface of first fθ lenses 406 and 606	d13 (mm)	8.20
Exit surface of first fθ lenses 406 and 606 - Incident surface of second fθ lenses 407 and 607	d14 (mm)	66.60
Incident surface of second fθ lenses 407 and 607 - Exit surface of second fθ lenses 407 and 607	d15 (mm)	4.30
Exit surface of second fθ lenses 407 and 607 - Second and fourth scanned surfaces 408 and 608	d16 (mm)	127.90
Deflection reference points D0 and E0 - Incident surface of first ff lenses 406 and 606	L3 (mm)	26.00
Deflection reference points D0 and E0 - Incident surface of second fθ lenses 407 and 607	L4 (mm)	100.80
Deflection reference points D0 and E0 - Second and fourth scanned surfaces 408 and 608	T2 (mm)	233.00
Sub-scanning eccentricity of second fθ lenses 407 and 607	shiftZ (mm)	5.96

Meridional line shape of first fθ lenses 406 and 606			Meridional line shape of second fθ lenses 407 and 607		
	Incident surface Opposite light source side	Exit surface Opposite light source side		Incident surface Opposite light source side	Exit surface Opposite light source side
R	−71.974	−43.211	R	−4000	345.598
ku	8.921E−01	−5.727E−01	ku	0	−9.021E+01
B4u	−7.612E−07	−1.995E−07	B4u	0	−2.166E−07
B6u	6.789E−09	1.645E−09	B6U	0	1.801E−11
B8u	−5.889E−12	1.272E−12	B8u	0	−1.069E−15
B10u	1.617E−15	−1.418E−15	B10u	0	2.983E−20
B12u	0	0	B12u	0	0
	Light source side	Light source side		Light source side	Light source side
k1	8.921E−01	−5.727E−01	k1	0	−9.021E+01
B41	−7.612E−07	−1.995E−07	B41	0	−2.166E−07
B61	6.789E−09	1.645E−09	B61	0	1.801E−11

TABLE 12-continued

B81	−5.889E−12	1.272E−12	B81	0	−1.069E−15
B101	1.617E−15	−1.418E−15	B101	0	2.983E−20
B121	0	0	B121	0	0
	Sagittal line shape of first fθ lenses 406 and 606			Sagittal line shape of second fθ lenses 407 and 607	
	Incident surface Sagittal line R change	Exit surface Sagittal line R change		Incident surface Sagittal line R change	Exit surface Sagittal line R change
r	20.000	20.586	r	26.855	294.0214
E1	0	0	E1	0	1.96971E−07
E2	0	1.558E−05	E2	−5.144E−06	−2.36769E−06
E3	0	0	E3	0	−3.44358E−09
E4	0	−3.394E−08	E4		−2.46843E−10
E5	0	0	E5	0	1.49969E−12
E6	0	3.964E−11	E6	0	1.69237E−14
E7	0	0	E7	0	−2.50442E−16
E8	0	−6.55816E−14	E8	0	−1.79515E−18
E9	0	0	E9	0	1.40544E−20
E10	0	5.40111E−17	E10	0	7.11738E−23
	Sagittal line tilt	Sagittal line tilt		Sagittal line tilt	Sagittal line tilt
M0_1	0	3.928E−02	M0_1	−1.514E−01	1.072E−02
M1_1	0	0	M1_1	−5.638E−06	2.983E−06
M2_1	0	−3.676E−05	M2_1	−2.604E−05	−4.002E−05
M3_1	0	0	M3_1	1.312E−07	1.175E−07
M4_1	0		M4_1	5.689E−09	7.909E−09
M5_1	0	0	M5_1	−3.827E−11	−3.145E−11
M6_1	0	0	M6_1	8.340E−14	−6.667E−13
M7_1	0	0	M7_1	5.134E−15	3.847E−15
M8_1	0	0	M8_1	−2.894E−17	8.307E−17
M9_1	0	0	M9_1	−2.202E−19	−1.374E−19
M10_1	0	0	M10_1	−5.517E−22	−5.821E−21
M11_1	0	0	M11_1	0	0
M12_1	0	0	M12_1	0	0

[0271] In Tables 10 to 12, an optical axis, an axis orthogonal to the optical axis in the main scanning cross section, and an axis orthogonal to the optical axis in the sub-scanning cross section are defined as an X-axis, a Y-axis and a Z-axis, respectively, when an intersection between each lens surface and the optical axis is defined as an origin. Further, in Tables 11 and 12, "E-x" means "$\times 10^{-x}$".

[0272] An aspherical shape (meridional line shape) in the main scanning cross section of each lens surface of the first fθ lenses **306**, **406**, **506** and **606** and the second fθ lenses **307**, **407**, **507** and **607** provided in the light scanning apparatus **910** according to the aspect of the embodiment is expressed by the above-described Expression (1).

[0273] An aspherical shape (sagittal line shape) in the sub-scanning cross section of each lens surface of the first fθ lenses **306**, **406**, **506** and **606** and the second fθ lenses **307**, **407**, **507** and **607** provided in the light scanning apparatus **910** according to the aspect of the embodiment is expressed by the above-described Expression (2).

[0274] A curvature radius r' in the sub-scanning cross section of each lens surface of the first fθ lenses **306**, **406**, **506** and **606** and the second fθ lenses **307**, **407**, **507** and **607** provided in the light scanning apparatus **910** according to the aspect of the embodiment continuously varies in accordance with a position in the Y direction as expressed by the above-described Expression (3).

[0275] Each of the first, second, third and fourth anamorphic collimator lenses **302**, **402**, **502** and **602** provided in the light scanning apparatus **910** according to the aspect of the embodiment has an incident surface formed by a diffracting surface defined by an optical path difference function of two variables Y and Z as expressed by the above-described Expression (4).

[0276] Further, in the first incident optical system **65***a* and the first scanning optical system **65***b* provided in the light scanning apparatus **910** according to the aspect of the embodiment, Inequality (11) be satisfied, Inequality (11a) be satisfied, and Inequality (11b) be satisfied.

[0277] Furthermore, in the first incident optical system **65***a* and the first scanning optical system **65***b* provided in the light scanning apparatus **910** according to the aspect of the embodiment, Inequalities (12) and (13) be satisfied.

[0278] Specifically, in the first incident optical system **65***a* and the first scanning optical system **65***b* provided in the light scanning apparatus **910** according to the aspect of the embodiment, β is −3.65, D is 34.2 mm, Lis 161.7 mm, and M is 0.138.

[0279] Therefore, the value of each of the Inequalities (11), (11a) and (11b) are calculated as 0.638, so that Inequalities (11) and (11a) are satisfied.

[0280] On the other hand, in the first incident optical system **65***a* and the first scanning optical system **65***b* provided in the light scanning apparatus **910** according to the aspect of the embodiment, M_{01} is 0.114.

[0281] Therefore, the value of the Inequality (12) is calculated as 0.527, so that Inequality (12) is not satisfied.

[0282] Further, in the first incident optical system **65**a and the first scanning optical system **65**b provided in the light scanning apparatus **910** according to the aspect of the embodiment, L_s is 1.31 mm, and R is 54.586 mm.

[0283] Therefore, the value of the Inequality (13) is calculated as 0.638, so that Inequality (13) is satisfied.

[0284] In the second incident optical system **75**a and the second scanning optical system **75**b provided in the light scanning apparatus **910** according to the aspect of the embodiment, Inequality (11) be satisfied, Inequality (11a) be satisfied, and Inequality (11b) be satisfied.

[0285] Further, in the second incident optical system **75**a and the second scanning optical system **75**b provided in the light scanning apparatus **910** according to the aspect of the embodiment, Inequalities (12) and (13) be satisfied.

[0286] Specifically, in the second incident optical system **75**a and the second scanning optical system **75**b provided in the light scanning apparatus **910** according to the aspect of the embodiment, β is −3.65, D is 34.2 mm, Lis 161.7 mm and M is 0.103.

[0287] Therefore, the value of each of the Inequalities (11), (11a) and (11b) is calculated as 0.476, so that Inequalities (11), (11a) and (11b) are satisfied.

[0288] Further, in the second incident optical system **75**a and the second scanning optical system **75**b provided in the light scanning apparatus **910** according to the aspect of the embodiment, M_{01} is 0.0393.

[0289] Therefore, the value of Inequality (12) is calculated as 0.182, so that Inequality (12) is satisfied.

[0290] Furthermore, in the second incident optical system **75**a and the second scanning optical system **75**b provided in the light scanning apparatus **910** according to the aspect of the embodiment, L_s is 1.31 mm, and R is 20.586 mm.

[0291] Therefore, the value of Inequality (13) is calculated as 0.476, and Inequality (13) is satisfied.

[0292] Further, in the third incident optical system **85**a and the third scanning optical system **85**b provided in the light scanning apparatus **910** according to the aspect of the embodiment, Inequality (11) be satisfied.

[0293] In other words, an inclination at the arrival position of the light beam from the k-th light emitting point of the third light source **501** on the exit surface (third sagittal line tilt surface, third optical surface) of the first fθ lens **506** provided in the light scanning apparatus **910** according to the aspect of the embodiment is represented by M_{3k}.

[0294] A lateral magnification in the sub-scanning cross section of the third incident optical system **85**a is represented by **β3**.

[0295] A distance on the optical axis of the third incident optical system **85**a between the third light source **501** and the second deflecting surface of the deflecting unit **1** provided in the light scanning apparatus **910** according to the aspect of the embodiment is represented by L_3 (mm).

[0296] A distance on the optical axis of the third scanning optical system **85**b between the second deflecting surface of the deflecting unit **1** and the exit surface of the first fθ lens **506** provided in the light scanning apparatus **910** according to the aspect of the embodiment is represented by D_3 (mm).

[0297] At this time, in the third incident optical system **85**a and the third scanning optical system **85**b provided in the light scanning apparatus **910** according to the aspect of the embodiment, the following Inequality (11e) be satisfied:

$$0.05 < \left| M_{3k}\left[-\beta_3 + \frac{(1-\beta_3)D_3}{L_3} \right] \right| < 0.70. \tag{11e}$$

[0298] Further, in the third incident optical system **85**a and the third scanning optical system **85**b provided in the light scanning apparatus **910** according to the aspect of the embodiment, Inequality (11a) be satisfied, and it is more preferred that Inequality (11b) be satisfied.

[0299] Furthermore, in the third incident optical system **85**a and the third scanning optical system **85**b provided in the light scanning apparatus **910** according to the embodiment, Inequalities (12) and (13) be satisfied.

[0300] Specifically, in the third incident optical system **85**a and the third scanning optical system **85**b provided in the light scanning apparatus **910** according to the aspect of the embodiment, β is −3.65, D is 34.2 mm, Lis 161.7 mm, and M is 0.138.

[0301] Therefore, the value of each of Inequalities (11), (11a) and (11b) is calculated as 0.638, so that Inequalities (11) and (11a) are satisfied.

[0302] On the other hand, in the third incident optical system **85**a and the third scanning optical system **85**b provided in the light scanning apparatus **910** according to the aspect of the embodiment, M_{01} is 0.114.

[0303] Therefore, the value of Inequality (12) is calculated as 0.527, so that Inequality (12) is not satisfied.

[0304] Further, in the third incident optical system **85**a and the third scanning optical system **85**b provided in the light scanning apparatus **910** according to the aspect of the embodiment, L_s is 1.31 mm, and R is 54.586 mm.

[0305] Therefore, the value of Inequality (13) is calculated as 0.638, so that Inequality (13) is satisfied.

[0306] In addition, in the fourth incident optical system **95**a and the fourth scanning optical system **95**b provided in the light scanning apparatus **910** according to the aspect of the embodiment, Inequality (11) be satisfied.

[0307] In other words, an inclination at the arrival position of the light beam from the 1-th light emitting point of the fourth light source **601** on the exit surface (fourth sagittal line tilt surface, fourth optical surface) of the first fθ lens **606** provided in the light scanning apparatus **910** according to the aspect of the embodiment is represented by M_{4l}.

[0308] A lateral magnification in the sub-scanning cross section of the fourth incident optical system **95**a is represented by $β_4$.

[0309] A distance on the optical axis of the fourth incident optical system **95**a between the fourth light source **601** and the second deflecting surface of the deflecting unit **1** provided in the light scanning apparatus **910** according to the aspect of the embodiment is represented by L_4 (mm).

[0310] A distance on the optical axis of the fourth scanning optical system **95**b between the second deflecting surface of the deflecting unit **1** and the exit surface of the first fθ lens **606** provided in the light scanning apparatus **910** according to the aspect of the embodiment is represented by D_4 (mm).

[0311] At this time, in the fourth incident optical system **95***a* and the fourth scanning optical system **95***b* provided in the light scanning apparatus **910** according to the aspect of the embodiment, the following Inequality (11f) be satisfied:

$$0.05 < \left| M_{4l}\left[-\beta_4 + \frac{(1-\beta_4)D_4}{L_4} \right] \right| < 0.70. \tag{11f}$$

[0312] Further, in the fourth incident optical system **95***a* and the fourth scanning optical system **95***b* provided in the light scanning apparatus **910** according to the aspect of the embodiment, Inequality (11a) be satisfied, and it is more preferred that Inequality (11b) be satisfied.

[0313] Furthermore, in the fourth incident optical system **95***a* and the fourth scanning optical system **95***b* provided in the light scanning apparatus **910** according to the aspect of the embodiment, Inequalities (12) and (13) be satisfied.

[0314] Specifically, in the fourth incident optical system **95***a* and the fourth scanning optical system **95***b* provided in the light scanning apparatus **910** according to the aspect of the embodiment, β is −3.65, D is 34.2 mm, Lis 161.7 mm, and M is 0.103.

[0315] Therefore, the value of each of Inequalities (11), (11a) and (11b) is calculated as 0.476, so that Inequalities (11), (11a) and (11b) are satisfied.

[0316] Further, in the fourth incident optical system **95***a* and the fourth scanning optical system **95***b* provided in the light scanning apparatus **910** according to the aspect of the embodiment, M_{01} is 0.0393.

[0317] Therefore, the value of Inequality (12) is calculated as 0.182, so that Inequality (12) is satisfied.

[0318] Furthermore, in the fourth incident optical system **95***a* and the fourth scanning optical system **95***b* provided in the light scanning apparatus **910** according to the aspect of the embodiment, L_s is 1.31 mm, and R is 20.586 mm.

[0319] Therefore, the value of Inequality (13) is calculated as 0.476, and Inequality (13) is satisfied.

[0320] As described above, in the light scanning apparatus **910** according to the aspect of the embodiment, Inequality (11) is satisfied in the first incident optical system **65***a* and the first scanning optical system **65***b*, thereby it is possible to suppress a deterioration in the image quality due to the deviation of the arrival position of each light beam on the first scanned surface **308**.

[0321] In the light scanning apparatus **910** according to the aspect of the embodiment, Inequality (11) is satisfied in the second incident optical system **75***a* and the second scanning optical system **75***b*, thereby it is possible to suppress a deterioration in the image quality due to the deviation of the arrival position of each light beam on the second scanned surface **408**.

[0322] In the light scanning apparatus **910** according to the aspect of the embodiment, Inequality (11) is satisfied in the third incident optical system **85***a* and the third scanning optical system **85***b*, thereby it is possible to suppress a deterioration in the image quality due to the deviation of the arrival position of each light beam on the third scanned surface **508**.

[0323] In the light scanning apparatus **910** according to the aspect of the embodiment, Inequality (11) is satisfied in the fourth incident optical system **95***a* and the fourth scanning optical system **95***b*, thereby it is possible to suppress a deterioration in the image quality due to the deviation of the arrival position of each light beam on the fourth scanned surface **608**.

[0324] Numerical values of the respective Inequalities in each of the light scanning apparatuses according to the first to fifth embodiments described above are shown in the following Table 13.

TABLE 13

	First embodiment	Second embodiment	Third embodiment
β	−3.65	−3.65	−3.65
D [mm]	34.2	34.2	34.2
L [mm]	161.7	161.7	161.7
M	−0.127	−0.0385	−0.0735
M01	−0.0918	−0.0385	−0.0212
Ls [mm]	−1.45	0	−1.31
R [mm]	41.166	76.858	25.004
Inequality (11): 0.05<| (−β + (1 − β) × D/L) × M|<0.70	0.589	0.179	0.341
Inequality (11a): 0.10<| (−β + (1 − β) × D/L) × M|<0.65			
Inequality (11b): 0.15<| (−β + (1 − β) × D/L) × M|<0.60			
Inequality (12): 0<| (−β + (1 − β) × D/L) × M01|<0.185	0.426	0.179	0.098
Inequality (13): 0.05<| (−β + (1 − β) × D/L) × (Ls/R + M01) |<0.70	0.589	0.179	0.341
1/R [1/mm]	0.0243	0.0130	0.0400

TABLE 13-continued

	Fourth embodiment		Fifth embodiment	
	First scanning system	Second scanning system	First and third scanning systems	Second and fourth scanning systems
β	−3.65	−3.65	−3.65	−3.65
D [mm]	34.2	34.2	34.2	34.2
L [mm]	161.7	161.7	161.7	161.7
M	0.100	0.0735	0.138	0.103
M01	0.0766	0.0212	0.114	0.0393
Ls [mm]	1.31	1.31	1.31	1.31
R [mm]	55.261	25.004	54.586	20.586
Inequality (11): $0.05<\|(-\beta+(1-\beta)\times D/L)\times M\|<0.70$	0.465	0.341	0.638	0.476
Inequality (11a): $0.10<\|(-\beta+(1-\beta)\times D/L)\times M\|<0.65$				
Inequality (11b): $0.15<\|(-\beta+(1-\beta)\times D/L)\times M\|<0.60$				
Inequality (12): $0<\|(-\beta+(1-\beta)\times D/L)\times M01\|<0.185$	0.355	0.098	0.527	0.182
Inequality (13): $0.05<\|(-\beta+(1-\beta)\times D/L)\times(Ls/R+M01)\|<0.70$	0.465	0.341	0.638	0.476
1/R [1/mm]	0.0181	0.0400	0.0183	0.0486

[0325] According to the aspect of the embodiments, a light scanning apparatus capable of easily reducing a deviation between scanning widths of multiple beams can be provided.

[0326] Although preferred embodiments have been described above, the disclosure is not limited to these embodiments, and various modifications and changes can be made within the scope of the gist of the disclosure.

[Image Forming Apparatus]

[0327] FIG. **16** shows a sub-scanning cross sectional view of a main part of an image forming apparatus **90** in which the light scanning apparatus **910** according to the fifth embodiment of the disclosure is mounted.

[0328] The image forming apparatus **90** is a tandem-type color image forming apparatus that records image information on a surface of each photosensitive drum serving as an image carrier by using the light scanning apparatus **910** according to the fifth embodiment.

[0329] The image forming apparatus **90** includes the light scanning apparatus **910** according to the fifth embodiment, developing units **15**, **16**, **17** and **18**, photosensitive drums (photosensitive bodies) **23**, **24**, **25** and **26**, a conveying belt **91**, a printer controller **93** and a fixing unit **94**.

[0330] Color signals (code data) of R (red), G (green) and B (blue) output from an external apparatus **92** such as a personal computer are input to the image forming apparatus **90**.

[0331] The input color signals are converted into image data (dot data) of C (cyan), M (magenta), Y (yellow), and K (black) by the printer controller **93** in the image forming apparatus **90**.

[0332] The converted image data is input to the light scanning apparatus **910** according to the fifth embodiment.

[0333] Light beams **19**, **20**, **21**, and **22** modulated in accordance with respective image data are emitted from the light scanning apparatus **910** according to the fifth embodiment, and photosensitive surfaces of photosensitive drums **23**, **24**, **25** and **26** are exposed to the light beams **19** to **22**.

[0334] In the image forming apparatus **90**, charging rollers (not shown) for uniformly charging the surfaces of the photosensitive drums **23** to **26** are provided so as to abut on the surfaces.

[0335] The surfaces of the photosensitive drums **23** to **26** charged by the charging rollers are irradiated with the light beams **19** to **22** from the light scanning apparatus **910** according to the fifth embodiment.

[0336] As described above, the light beams **19** to **22** are modulated on the basis of the image data of the respective colors, and electrostatic latent images are formed on the surfaces of the photosensitive drums **23** to **26** by the irradiation with the light beams **19** to **22**.

[0337] The formed electrostatic latent images are developed as toner images by developing units **15**, **16**, **17** and **18** arranged so as to abut on the photosensitive drums **23** to **26**.

[0338] The toner images developed by the developing units **15** to **18** are multi-transferred onto a sheet (transferred material) (not shown) conveyed on the conveying belt **91** by a transferring roller (transferring unit) (not shown) arranged so as to face the photosensitive drums **23** to **26**, thereby forming one full-color image.

[0339] Then, the sheet on which the unfixed toner image is transferred is further conveyed to the fixing unit **94** arranged behind the photosensitive drums **23** to **26** (on the left side in FIG. **16**).

[0340] The fixing unit **94** is formed by a fixing roller having a fixing heater (not shown) therein and a pressurizing roller arranged so as to be in pressure contact with the fixing roller.

[0341] Then, the sheet conveyed from the transferring portion is heated while being pressed at the pressure-contact portion between the fixing roller and the pressurizing roller, thereby the unfixed toner image on the sheet is fixed.

[0342] Further, a sheet discharging roller (not shown) is arranged behind the fixing roller, and the sheet discharging roller discharges the sheet on which the toner image is fixed to the outside of the image forming apparatus **90**.

[0343] The image forming apparatus **90** records image signals (image information) on the photosensitive surfaces of the photosensitive drums **23** to **26** corresponding to the respective colors of C, M, Y and K by using the light scanning apparatus **910** according to the fifth embodiment, and prints a color image at high speed.

[0344] As the external apparatus **92**, for example, a color image reading apparatus including a CCD sensor may be used. In this case, the color image reading apparatus and the image forming apparatus **90** form a color digital copying machine.

[0345] The image forming apparatus **90** may be provided with four light scanning apparatuses according to any one of the first to third embodiments or two light scanning apparatuses **710** according to the fourth embodiment instead of the light scanning apparatus **910** according to the fifth embodiment.

[0346] While the embodiments of the disclosure have been described with reference to exemplary embodiments, it is to be understood that the disclosure is not limited to the disclosed exemplary embodiments. The scope of the following claims is to be accorded the broadest interpretation so as to encompass all such modifications and equivalent structures and functions.

[0347] This application claims the benefit of Japanese Patent Application No. 2024-019123, filed Feb. 13, 2024, which is hereby incorporated by reference herein in its entirety.

What is claimed is:

1. An apparatus comprising:

a deflecting unit configured to deflect a plurality of light fluxes from a first light source with a plurality of light emitting points to scan a first scanned surface in a main scanning direction;

a first element having a first surface and configured to guide the plurality of light fluxes deflected by a first deflecting surface of the deflecting unit to the first scanned surface; and

a first incident system configured to cause the plurality of light fluxes from the first light source to be incident on the first deflecting surface,

wherein, a following condition is satisfied:

$$0.05 < \left| M_{1i}\left[-\beta_1 + \frac{(1-\beta_1)D_1}{L_1}\right] \right| < 0.70,$$

where L_1 represents a distance between the first light source and the first deflecting surface on an optical axis of the first incident system, D_1 represents a distance between the first deflecting surface and the first surface on an optical axis of the first element, β_1 represents a lateral magnification in a sub-scanning cross section of the first incident system, and M_{1i} represents an inclination of the first surface at a position at which the light flux from an i-th light emitting point of the first light source arrives on the first surface.

2. The apparatus according to claim **1**, wherein a following condition is satisfied:

$$0 < \left| M_{01}\left[-\beta_1 + \frac{(1-\beta_1)D_1}{L_1}\right] \right| < 0.185,$$

where M_{01} represents a sagittal line tilt amount of the first surface on the optical axis of the first element.

3. The apparatus according to claim **1**, wherein a following condition is satisfied:

$$0.05 < \left| \left[\frac{L_s}{R} + M_{01}\right] \times \left[-\beta_1 + \frac{(1-\beta_1)D_1}{L_1}\right] \right| < 0.70,$$

where R represents a curvature radius in the sub-scanning cross section of the first surface on the optical axis of the first element, L_s represents an eccentricity amount in a sub-scanning direction of the first element, and M_{01} represents a sagittal line tilt amount of the first surface on the optical axis of the first element.

4. The apparatus according to claim **1**, wherein a sagittal line tilt amount of the first surface varies in accordance with a position in the main scanning direction.

5. The apparatus according to claim **4**, wherein an absolute value of a sagittal line tilt amount of the first surface is largest on the optical axis of the first element.

6. The apparatus according to claim **1**, wherein the first element has a positive power in the sub-scanning cross section.

7. The apparatus according to claim **1**, further comprising a first imaging system including the first element and configured to guide the plurality of light fluxes deflected by the first deflecting surface to the first scanned surface,

wherein an element closest to the deflecting unit on the paths of the plurality of light fluxes among at least one element included in the first imaging system is an element having the strongest power in a main scanning cross section among the at least one element.

8. The apparatus according to claim **1**, further comprising:

a second element having a second surface and configured to guide a plurality of light fluxes of a second light source with a plurality of light emitting points deflected by the first deflecting surface to a second scanned surface; and

a second incident system configured to cause the plurality of light fluxes from the second light source to be incident on the first deflecting surface,

wherein the deflecting unit is configured to deflect the plurality of light fluxes from the second light source to scan the second scanned surface in the main scanning direction, and

wherein, a following condition is satisfied:

$$0.05 < \left| M_{2j}\left[-\beta_2 + \frac{(1-\beta_2)D_2}{L_2}\right] \right| < 0.70,$$

where L_2 represents a distance between the second light source and the first deflecting surface on an optical axis of the second incident system, D_2 represents a distance between the first deflecting surface and the second surface on an optical axis of the second element, β_2 represents a lateral magnification in the sub-scanning cross section of the second incident system, and M_{2j} represents an inclination of the second surface at a position at which the light flux from a j-th light emitting point of the second light source arrives on the second surface.

9. The apparatus according to claim **8**, wherein an absolute value of a sagittal line tilt amount of the first surface on the optical axis of the first element and an absolute value of a sagittal line tilt amount of the second surface on the optical axis of the second element are different from each other.

10. The apparatus according to claim **8**, further comprising:

a third element having a third surface and configured to guide a plurality of light fluxes of a third light source with a plurality of light emitting points deflected by a second deflecting surface of the deflecting unit to a third scanned surface;

a fourth element having a fourth surface and configured to guide a plurality of light fluxes of a fourth light source with a plurality of light emitting points deflected by the second deflecting surface to a fourth scanned surface;

a third incident system configured to cause the plurality of light fluxes from the third light source to be incident on the second deflecting surface; and

a fourth incident system configured to cause the plurality of light fluxes from the fourth light source to be incident on the second deflecting surface,

wherein the deflecting unit is configured to deflect the plurality of light fluxes from the third light source and the plurality of light fluxes from the fourth light source to scan the third and fourth scanned surfaces in the main scanning direction, respectively,

wherein, a following condition is satisfied:

$$0.05 < \left| M_{3k}\left[-\beta_3 + \frac{(1-\beta_3)D_3}{L_3} \right] \right| < 0.70,$$

where L_3 represents a distance between the third light source and the second deflecting surface on an optical axis of the third incident system, D_3 represents a distance between the second deflecting surface and the third surface on an optical axis of the third element, β_3 represents a lateral magnification in the sub-scanning cross section of the third incident system, and M_{3k} represents an inclination of the third surface at a position at which the light flux from a k-th light emitting point of the third light source arrives on the third surface, and

wherein, a following condition is satisfied:

$$0.05 < \left| M_{4l}\left[-\beta_4 + \frac{(1-\beta_4)D_4}{L_4} \right] \right| < 0.70,$$

where L_4 represents a distance between the fourth light source and the second deflecting surface on an optical axis of the fourth incident system, D_4 represents a distance between the second deflecting surface and the fourth surface on an optical axis of the fourth element, β_4 represents a lateral magnification in the sub-scanning cross section of the fourth incident system, and M_{4l} represents an inclination of the fourth surface at a position at which the light flux from an l-th light emitting point of the fourth light source arrives on the fourth surface.

11. An apparatus comprising:

a deflecting unit configured to deflect a plurality of light fluxes from a first light source with a plurality of light emitting points to scan a first scanned surface in a main scanning direction;

a first element having a first surface and configured to guide the plurality of light fluxes deflected by a first deflecting surface of the deflecting unit to the first scanned surface; and

a first incident system configured to cause the plurality of light fluxes from the first light source to be incident on the first deflecting surface,

wherein a normal of the first surface on an optical axis of the first element is inclined with respect to the optical axis.

12. A forming apparatus comprising:

the apparatus according to claim **1**; and

a developing unit configured to develop an electrostatic latent image formed on the first scanned surface by the apparatus.

13. The forming apparatus according to claim **12**, wherein, in the apparatus, a following condition is satisfied:

$$0 < \left| M_{01}\left[-\beta_1 + \frac{(1-\beta_1)D_1}{L_1} \right] \right| < 0.185,$$

where M_{01} represents a sagittal line tilt amount of the first surface on the optical axis of the first element.

14. The forming apparatus according to claim **12**, wherein, in the apparatus, a following condition is satisfied:

$$0.05 < \left| \left[\frac{L_s}{R} + M_{01} \right] \times \left[-\beta_1 + \frac{(1-\beta_1)D_1}{L_1} \right] \right| < 0.70,$$

where R represents a curvature radius in the sub-scanning cross section of the first surface on the optical axis of the first element, L_s represents an eccentricity amount in a sub-scanning direction of the first element, and M_{01} represents a sagittal line tilt amount of the first surface on the optical axis of the first element.

15. The forming apparatus according to claim **12**, wherein, in the apparatus, a sagittal line tilt amount of the first surface varies in accordance with a position in the main scanning direction.

16. The forming apparatus according to claim **15**, wherein, in the apparatus, an absolute value of a sagittal line tilt amount of the first surface is largest on the optical axis of the first element.

17. A forming apparatus comprising:

the apparatus according to claim **1**; and

a controller configured to convert a signal output from an external apparatus into image data to input the image data to the apparatus.

18. The forming apparatus according to claim **17**, wherein, in the apparatus, a following condition is satisfied:

$$0 < \left| M_{01}\left[-\beta_1 + \frac{(1-\beta_1)D_1}{L_1} \right] \right| < 0.185,$$

where M_{01} represents a sagittal line tilt amount of the first surface on the optical axis of the first element.

19. The forming apparatus according to claim **17**, wherein, in the apparatus, a following condition is satisfied:

$$0.05 < \left| \left[\frac{L_s}{R} + M_{01} \right] \times \left[-\beta_1 + \frac{(1-\beta_1)D_1}{L_1} \right] \right| < 0.70,$$

where R represents a curvature radius in the sub-scanning cross section of the first surface on the optical axis of the first element, L_s represents an eccentricity amount in a sub-scanning direction of the first element, and M_{01} represents a sagittal line tilt amount of the first surface on the optical axis of the first element.

20. The forming apparatus according to claim **17**, wherein, in the apparatus, a sagittal line tilt amount of the first surface varies in accordance with a position in the main scanning direction.

* * * * *